SUPPLEMENTARY INFORMATION

Discovery of a chemical probe for the L3MBTL3 methyl-lysine reader domain

James, Lindsey I.[1]; Barsyte-Lovejoy, Dalia[2]; Zhong, Nan[2]; Krichevsky, Liubov[2,3,4]; Korboukh, Victoria K.[1]; Herold, J. Martin[1]; MacNevin, Christopher J.[1,8]; Norris, Jacqueline L.[1]; Sagum, Cari A.[5]; Tempel, Wolfram[2]; Marcon, Edyta[6]; Guo, Hongbo[6]; Gao, Cen[1]; Huang, Xi-Ping[7,8]; Duan, Shili[4]; Emili, Andrew[6]; Greenblatt, Jack F.[6]; Kireev, Dmitri B.[1]; Jin, Jian[1]; Janzen, William P.[1]; Brown, Peter J.[2]; Bedford, Mark T.[5]; *Arrowsmith, Cheryl H.[2,3,4]; *Frye, Stephen V.[1]

[1]Center for Integrative Chemical Biology and Drug Discovery, Division of Chemical Biology and Medicinal Chemistry, UNC Eshelman School of Pharmacy, University of North Carolina at Chapel Hill, Chapel Hill, North Carolina 27599, USA. [2]Structural Genomics Consortium, University of Toronto, Toronto, Ontario, M5G 1L7, Canada. [3]Department of Medical Biophysics, University of Toronto, 101 College Street, Toronto, Ontario, M5G 1L7, Canada. [4]Ontario Cancer Institute and Campbell Family Cancer Research Institute, University of Toronto, 101 College Street, Toronto, Ontario, M5G 1L7, Canada. [5]M. D. Anderson Cancer Center Department of Carcinogenesis, University of Texas, Smithville, TX, USA. [6]Banting and Best Department of Medical Research, Donnelly Centre, 160 College Street, Toronto, ON, M5S 3E1. [7]National Institute of Mental Health Psychoactive Drug Screening Program, University of North Carolina at Chapel Hill Medical School, Chapel Hill, North Carolina 27599, USA. [8]Department of Pharmacology, University of North Carolina at Chapel Hill Medical School, Chapel Hill, North Carolina 27599, USA.

*e-mail: svfrye@email.unc.edu or carrow@uhnres.utoronto.ca

Supplementary Methods

Protein mutagenesis. L3MBTL3 mutants were generated from a pET28-mhl vector encoding the three MBT domains (residues 225-555, reference sequence AAH60845) using the following primer sets:

D274A sense primer 5'-GAAATTAGAAGGCGTGGCTCCTGAGCATCAGTCTG-3'
antisense primer 5'-CAGACTGATGCTCAGGAGCCACGCCTTCTAATTTC-3';
H277A sense primer 5'-GGCGTGGATCCCGAGGCTCAGTCTGTGTACTG-3'
antisense primer 5'-CAGTACACAGACTGAGCCTCGGGATCCACGCC-3';
D381A sense primer 5'-ATGAAGCTTGAGGCAGTAGCCAAAAAGAATCCCTCATTC-3'
antisense primer 5'-GAATGAGGGATTCTTTTTGGCTACTGCCTCAAGCTTCAT-3';
F387L sense primer 5'-AGACAAAAAGAATCCCTCATTAATCTGTGTTGCTACGGTAAC-3'
antisense primer 5'-GTTACCGTAGCAACACAGATTAATGAGGGATTCTTTTTGTCT-3';
D485A sense primer 5'-AAAAATGAAGCTTGAGGTTGTAGCCAAAAGGAACCCTATGTTTATTA-3'
antisense primer 5'-TAATAAACATAGGGTTCCTTTTGGCTACAACCTCAAGCTTCATTTTT-3'.

Mutagenesis reactions were performed with QuickChange II site directed mutagenesis kit (Agilent Technologies, Santa Clara, CA) according to the manufacture's recommendations.

Protein expression and purification. L3MBTL1, L3MBTL3 and all L3MBTL3 mutants were purified essentially as described.[1] Briefly, cell pellets from 2 L cultures expressing His-tagged proteins were lysed with BugBuster protein extraction reagent (EMD Millipore, Darmstadt, Germany) containing 20 mM imidazole. The cell lysate was clarified by centrifugation and loaded onto a 5 mL HisTrap HP column (GE Healthcare, Piscataway, NJ) equilibrated with binding and wash buffer (50 mM sodium phosphate buffer pH 7.2, 500 mM NaCl, 30 mM imidazole) using an ÄKTA FPLC (GE Healthcare, Piscataway, NJ) at 1 mL/min. His-tagged protein was eluted using a linear gradient of elution buffer (50 mM sodium phosphate buffer pH 7.2, 500 mM NaCl, 500 mM imidazole) over 20 column volumes. Fractions containing the desired protein were confirmed by SDS-PAGE, pooled and loaded at 2 mL/min onto a HiLoad 26/60 Superdex 200 prep grade size exclusion column (GE Healthcare, Piscataway, NJ) using an ÄKTA FPLC. A constant flow of 2 mL/min size exclusion buffer (25 mM Tris·HCl pH 8.0, 250 mM NaCl, 1 mM EDTA, 2 mM DTT, 0.02% Tween 20) was used to elute proteins. Fractions containing the desired protein were identified by SDS-PAGE, pooled and subjected to simultaneous concentration and buffer exchange using an Amicon Ultra-15 centrifugal filter unit (Millipore, Billerica, MA) and storage buffer (20 mM Tris·HCl pH 8.0, 150 mM NaCl and 2 mM DTT for L3MBTL1 and 20 mM Tris HCl, pH 8.0, 250 mM

NaCl and 2 mM DTT for L3MBTL3 wild type and mutant proteins). Protein concentration was determined by absorbance at 280 nm using the Edelhoch method[2] and protein purity was determined to be >95% by Coomassie. The L3MBTL3 D485A mutant was expressed but the resulting protein did not bind to the nickel resin.

A pET28-mhl vector containing the coding region for residues 1-455 of SFMBT1 (reference sequence AAH14614) was transformed into BL21 Codon Plus cells (Agilent Technologies, Santa Clara, CA). A 2 L culture was grown to mid log phase at 37 °C then the temperature was lowered to 18 °C and protein expression was induced by addition of 0.5 mM IPTG. Expression was allowed to continue overnight. SFMBT1 protein was purified essentially as described above except for the use of a buffer consisting of 25 mM Tris HCl pH 7.5, 250 mM NaCl, and 1 mM DTT for size exclusion chromatography and protein storage.

A pET28-mhl vector containing the coding region for residues 1485-1611 of 53BP1 (reference sequence (NP_001135452) was transformed into BL21 Rosetta DE3 pLysS cells (EMD Millipore). A 2 L culture was grown to mid log phase at 37 °C then the temperature was lowered to 18 °C and protein expression was induced by addition of 0.5 mM IPTG. Expression was allowed to continue overnight. 53BP1 protein was purified essentially as described above except for the use of a buffer consisting of 25 mM Tris HCl pH 7.5, 150 mM NaCl, and 2 mM DTT for size exclusion chromatography and protein storage.

A pET28 vector containing the coding region for residues 121-286 of UHRF1 (reference sequence (NP_001041666) was transformed into BL21 Rosetta DE3 pLysS cells (EMD Millipore). A 2 L culture was grown to mid log phase at 37 °C then the temperature was lowered to 18 °C and protein expression was induced by addition of 0.5 mM IPTG. Expression was allowed to continue overnight. UHRF1 protein was purified exactly as described for 53BP1.

pGEX expression vectors for all of the following proteins were obtained from the Bedford lab and transformed into BL21 Rosetta DE3 pLysS cells (EMD Millipore): GST-53BP1 Tudor (residues 1459-1634, reference sequence NP_005648), SPF30 Tudor (residues 25-162, reference sequence NP_588166), PHF20 Tudor (residues 58-148, reference sequence NP_057520), PHF20L1 Tudor (residues 61-160, reference sequence NM_016018), PHF20L1 MBT (residues 1-74, reference sequence NP_057102), and MRG15 (residues 1-79, reference sequence AAD29872). A 2L culture of each protein was grown to mid log phase at 37°C then the temperature was lowered to 18°C and protein expression was induced by the addition of 0.5mM IPTG. Expression was allowed to continue overnight. Cell pellets from each 2 L

cultures expressing GST-tagged proteins were lysed with BugBuster protein extraction reagent (EMD Millipore, Darmstadt, Germany) containing 5mM DTT. The cell lysate was clarified by centrifugation and loaded onto a 5 mL GSTrap FF column (GE Healthcare, Piscataway, NJ) equilibrated with binding and wash buffer (1XPBS, 5mM DTT) using an ÄKTA FPLC (GE Healthcare, Piscataway, NJ) at 1 mL/min. The column was washed with 10 column volumes of binding and wash buffer and GST-tagged protein was eluted in a buffer containing 50mM Tris pH 7.5, 150mM NaCl, 10mM reduced glutathione. Protein was collected in 1ml fractions over 10 column volumes and fractions containing the desired protein were confirmed by SDS-PAGE, pooled and loaded at 2 mL/min onto a HiLoad 26/60 Superdex 200 prep grade size exclusion column (GE Healthcare, Piscataway, NJ) using an ÄKTA FPLC. A constant flow of 2 mL/min size exclusion buffer (25 mM Tris·HCl pH 8.0, 150 mM NaCl, 2 mM DTT) was used to elute proteins. Fractions containing the desired protein were identified by SDS-PAGE, pooled and concentrated using Amicon Ultra-15 centrifugal filter units (Millipore, Billerica, MA). Protein concentration was determined by absorbance at 280 nm using the Edelhoch method and protein purity was determined to be >95% by Coomassie.

The identity of all expression constructs was verified by DNA sequencing and all proteins were at least 95% pure as determined by Coomassie staining. L3MBTL4, MBTD1 and CBX7 proteins were provided by the Structural Genomics Consortium. PHF23 and JARID1A proteins were provided by Greg Wang (UNC).

AlphaScreen assay. The AlphaScreen assay was performed as described elsewhere.[1,3] In brief, compound plates (1 µL at 10 or 30 mM highest concentration) were diluted in 1X assay buffer (20 mM TRIS pH 8.0, 25 mM NaCl, 2 mM DTT and 0.05% Tween-20) over 2 steps using a Multimek robotic pipettor (Nanoscreen) and 1 µL was spotted into the wells of 384-well assay Proxiplates (PerkinElmer). To these plates 9 µL of protein- peptide mix in 1X assay buffer was added by Multidrop (Thermo) and incubated for 30 min at room temperature. At this point 2 uL of streptavidin- conjugate donor and nickel-chelate acceptor beads (45 µg/mL in 1X assay buffer) were added, the plates were allowed to incubate for an additional 30 min in the dark at room temperature. After incubation the plates were read on EnVision mulilabel reader equipped with HTS alpha screen laser (Perkin Elmer). The screens reported are performed up to 10 or 30 µM, and therefore it should be noted that those compounds referred to as inactive are indeed inactive only within the concentration range tested. PHF23 and JARID1A were GST tagged and consequently for these assays GST-acceptor beads were used. It should be noted that any positive binding curves for L3MBTL4 that were generated yielded curves with very shallow slopes, suggesting a nonspecific interaction.

The data for the IC_{50} values was calculated from replicate runs (see n values in **Supplementary Table 1**), in that the datapoints for each compound concentration were averaged and plotted using 4-parameters curve fitting (GraphPad Prism 5).

ITC experiments. All ITC measurements were recorded at 25 °C with an AutoITC200 microcalorimeter (MicroCal Inc., MA). All protein and compound stock samples were in the target buffer (25 mM Tris-HCl, pH 8, 75-150 mM NaCl, and 2 mM β-mercaptoethanol), and then diluted in the same buffer to achieve the desired concentrations: 30 – 95 μM protein and 0.3 – 1 mM compound. The concentration of the protein stock solutions was established using the Edelhoch method, whereas 10 mM compound stock solutions were prepared gravimetrically based on molecular weight. A typical experiment included a single 0.2 μL compound injection into a 200 μL cell filled with protein, followed by 26 subsequent 1.5 μL injections of compound. Injections were performed with a spacing of 180 seconds and a reference power of 8 μcal/sec. Control experiments were performed titrating each compound into buffer under identical conditions to determine the heat signals, if any, that arise from diluting the compound. If applicable, the heats of dilution generated were then subtracted from the protein-compound binding curves. The titration data was analyzed using Origin Software (MicroCal Inc., USA) by non-linear least squares, fitting the heats of binding as a function of the compound:protein ratio. The data was fit based on a one set of sites model. L3MBTL3 binding was also fit based on one site due to the fact that two binding events were not observed, and therefore the data could not be fit based on two independent or sequential binding events.

It should be noted that due to the high concentrations of proteins required for these experiments, it was sometimes difficult to maintain complete solubility. When insoluble material was apparent, the protein was spun down, the soluble protein was decanted, and the concentration was re-determined prior to beginning the experiment. However it is foreseeable that protein precipitation during titrations may affect the determined binding stoichiometry, and we believe this is the reason for observed N values that are less than anticipated in some cases. Furthermore, we were unable to achieve saturation at the beginning of the ITC binding curves in the case of the weaker binders (L3MBTL1, 53BP1, PHF20, PHF20L1, SPF30, MRG15) making it impractical to accurately determine the N value of binding. In the case of PHF20, a recent report shows that the second tudor domain forms a stable homodimer cross-linked by two disulfide bonds, and this may also serve to influence the observed binding stoichiometry for this protein.[4]

Size exclusion experiments. L3MBTL3 3MBT was cloned into pNIC-CH which is a pET expression vector with C-terminal Hexa-His tag (GenBank GI number 5729993). The protein was expressed in *E.coli* BL21 (DE3) strain (EMD Biosciences) in Terrific Broth (TB) and was purified using metal affinity chromatography on a Ni-chelating open column followed by a cation-exchange chromatography on a HiTrap SP HP column and a size exclusion chromatography on a pre-packed HiLoad 16/60 Superdex 200 pg size exclusion column (GE Life Sciences).

Protein array experiments. The generation of CADOR protein microarrays and peptide probe preparation have been described previously.[5] A list of the protein domains on this array has been published.[6]

Histone methyltransferase selectivity assays. Selectivity experiments for UNC1215 using different HMTs (G9a, EHMT1, SUV39H2, PRMT3, SETD7, SETD8, and PRMT5, PRC2 and MLL complexes) were performed by monitoring the incorporation of tritium-labeled methyl group from SAM to lysine or arginine residues of peptide substrates (corresponding amino acids of histone tails) using Scintillation Proximity Assay (SPA). The enzymatic reactions were conducted in triplicate at room temperature with 1 hour incubation of a 20 µL reaction mixture in 20 mM Tris pH 8.0, 5 mM DTT, and 0.01% Triton X-100 containing ^{3}H-SAM (Cat.# NET155V250UC; Perkin Elmer; www.perkinelmer.com) at saturation for each enzyme. The protein concentration in the assay for each HMT was as follows: G9a (10 nM), EHMT1 (10 nM), SUV39H2 (20 nM), PRMT3 (100 nM), SETD7 (20 nM), SETD8 (50 nM), PRMT5 complex (PRMT5/MEP50; 200 nM), PRC2 complex (EZH2/EED/SUZ12; 50 nM), and MLL complex (MLL/WDR5/RbBP5; 1 µM). The concentration of biotinylated peptides in each assay was as follows: H3 (1-25) for G9a (0.8µM), EHMT1 (0.6 µM), SUV39H2 (0.5 µM), SETD7 (19 µM) and MLL complex (2 µM); H3 (21-44) for PRC2 complex (1 µM); and H4 (1-24) for PRMT3 (0.6 µM), PRMT5 complex (2 µM) and SETD8 (40 µM). IC_{50} values were determined using compound concentrations ranging from 250 nM to 250 µM. To stop the enzymatic reactions, 20 µL of 7.5 M guanidine hydrochloride was added, followed by 180 µL of buffer (20 mM Tris, pH 8.0). The reactions were mixed and then transferred to a 96-well FlashPlate (Cat.# SMP103; Perkin Elmer; www.perkinelmer.com). After mixing, the reaction mixtures in Flash plate were incubated for 1 hour and the CPM counts were measured using Topcount plate reader (Perkin Elmer, www.perkinelmer.com). The CPM counts in the absence of compound for each data set were defined as 100% activity. In the absence of the enzyme, the CPM counts in each data set were defined as background (0%). The IC_{50} values were determined using SigmaPlot software. For DNMT1, the IC_{50} determination was performed as described above by using dsDNA as a substrate. The dsDNA

substrate was prepared by annealing two complementary strands (biotinylated forward strand: B-GAGCCCGTAAGCCCGTTCAGGTCG and reverse strand: CGACCTGAACGGGCTTACGGGCTC), synthesized by Eurofins MWG Operon. DNMT1 (100 nM) was incubated with dsDNA substrate (100 nM), ^{3}H-SAM (2 µM, ~ 60 µCi/mL) in buffer (20 mM Tris-HCl, pH 8.0, 5 mM DTT, 0.01% Triton X-100) and the reactions were incubated for 1 hour at 37 °C before quenching.

Bromodomain and lysine demethylase selectivity assays. Thermal melting experiments were carried out using an Mx3005p Real Time PCR machine (Stratagene).[7] Proteins were buffered in 10 mM HEPES pH 7.5, 500 mM NaCl and assayed in a 96-well plate at a final concentration of 1 µM (demethylases) or 2 µM (bromodomains) in 20 µl volume. Compounds were added at a final concentration of 20 µM (demethylases) or 10 µM (bromodomains). SYPRO Orange (Molecular Probes) was added as a fluorescence probe at a dilution of 1:1000. Excitation and emission filters for the SYPRO-Orange dye were set to 465 and 590 nm, respectively. The temperature was raised with a step of 3 °C per minute from 25 °C to 96 °C and fluorescence readings were taken at each interval.

NIMH PDSP selectivity assays. Selectivity of UNC1215 against the targets in the NIMH PDSP selectivity panel was performed by the NIMH PDSP at University of North Carolina at Chapel Hill (http://pdsp.med.unc.edu/) in radioligand binding assays.

Protocols of the M_1 Ca^{2+} mobilization assay are available from the NIMH PDSP website: http://pdsp.med.unc.edu/UNC-CH%20Protocol%20Book.pdf.

Protocols of M_2 cAMP biosensor assays: HEK293T cells co-transfected with the cAMP biosensor GloSensor-22F (Promega) and hM_2 were seeded (20,000 cells/40 µL/well) into poly-L-Lysine coated 384-well white, clear-bottom, tissue culture plates in DMEM with 1% dialyzed FBS for overnight. Before the assay, media was removed and cells were loaded with 4mM luciferin (20 µL/well) in drug buffer (1x HBSS, 20 mM HEPES, pH 7.4) for 90 min at 37°C. For agonist activity, cells were first treated with UNC1215 for 10 min, followed by addition of 200 nM isoproterenol for another 10 min. For antagonist activity, cells were first treated with UNC1215 for 10 min, followed by 100 nM acetylcholine for 10 min, then 200 nM isoproterenol for 10 min. Luminescence per well per second was read on a Wallac TriLux microbeta plate counter. Data were normalized to the isoproterenol response (0%) and the maximal atropine-induced inhibition thereof (0%) and regressed using the sigmoidal dose-response function built into GraphPad Prism 5.0.

Schild analysis. The antagonist potency of UNC1215 against endogenous agonist acetylcholine at hM_1 or hM_2 was determined by measuring acetylcholine dose-responses in the absence and presence of a serial dilution of UNC1215 concentrations (from 30 nM to 30 μM). Results were normalized (acetylcholine maximum activity as 100% and buffer control as 0%) and analyzed using a modified Lew-Angus method[8] with GraphPad Prism 5.0.

Kinase selectivity assays. Selectivity of UNC1215 against a kinase panel (**Supplementary Table 5**) was performed by Carna Biosciences. Assay protocols are available at https://www.carnabio.com/english/product/search.cgi?mode=profiling.

CellTiter-Glo Luminescent Cell Viability Assay. The effect of UNC1215, UNC1021, and UNC1079 on cell viability was determined using a modified CellTiter-Glo™ ATP detection system (Promega #7573). Ten point, 1:3 dilution curves of compounds starting at 100 μM final concentration were diluted to 5X final concentration in PBS (vehicle control) and then 5 μL were added to 384-well white, clear bottom tissue culture plates (Corning #3707) with a Multimek automated liquid handling device (Nanoscreen, Charleston, SC). Twenty microliters of low passage, subconfluent HEK293T/17 cells (ATCC CRL-11268) grown in Dulbecco's Modified Eagle's Medium without phenol red (Gibco #31053) and supplemented with 10% Fetal Bovine Serum (Gibco #26140) were immediately added at a density of 5,000 cells per well using a Multidrop 384 (Titertek). Cell plates were incubated for 24 hours at 37°C and 5% $C0_2$, and then lysed with 25 microliters of CellTiter-Glo™ reagent. Luminescence was read on an Envision platereader (Perkin Elmer) after 15 minutes at room temperature in dim light.

Stability of UNC1215 in a buffer stock solution. A 10 mM solution of UNC1215 in 25 mM Tris-HCl, pH 8, 150 mM NaCl, and 2 mM β-mercaptoethanol was prepared and kept at room temperature for 4 weeks. The solution was monitored weekly by LCMS to assess the stability of UNC1215, and no changes were observed, indicating high stability under these conditions.

Stability of UNC1215 under cellular assay conditions. HEK293T cells were grown in Dulbecco's Modified Eagle's Medium (DMEM) without phenol red (Gibco 31053) supplemented with 10% FBS (Hyclone AWD11518). At the time of compound treatment (time 0), approximately 1 X 10^5 cells/ml or media alone was supplemented with 500 μM UNC1215 or the equivalent buffer vehicle in triplicate. All samples were incubated at 37°C/5% CO_2. At time 0, and after 24 and 48 hours, media was collected from the samples and centrifuged to remove any cell debris. 20 μl from each of the samples was mixed with 80 μl of HPLC grade methanol in a 384 well deep well plate (Greiner), heat sealed, vortexed, and

spun to remove any residue. 50 µl of the resulting 'supernatant' was transferred to a new 384 well plate, sealed, and analyzed using an Agilent 6110 LCMS Series system with the UV detector set to at 254 nm. Samples were injected (20 µl) onto an Agilent Eclipse Plus 4.6 × 50 mm, 1.8 µm, C18 column at room temperature, using mobile phases A (H_2O + 0.1% acetic acid) and B (MeOH + 0.1% acetic acid) and a linear gradient from 10% to 100% B in 5.0 min with a flow rate of 1.0 mL/min. Mass spectra (MS) data were acquired in positive ion mode using an Agilent 6110 single quadrupole mass spectrometer with an electrospray ionization (ESI) source. No degradation products of UNC1215 were observed for any of the treatment groups.

Cell lines and cell culture. Media was purchased from Gibco. The HEK293 cell line was cultured in high glucose DMEM medium (11960) and U2OS cells in RPMI, all supplemented with 10% FBS, 1% glutamine, and 1% penicillin-streptomycin.

Cloning and mutagenesis. L3MBTL3 cDNA was PCR amplified using MGC clone corresponding to NP_001007103.1 and subsequently cloned into pACGFP C3, pACGFP N3, or pmCherry (Clontech), or pCDNA3-Flag (Invitrogen) using standard cloning procedures. Site directed mutagenesis was performed with Quick change (Stratagene).

Supplementary Results

Supplementary Figure 1. AlphaScreen binding curves.

a) **Averaged AlphaScreen binding curves for UNC1021, UNC1215, and UNC1079 against L3MBTL3 (3MBT).** UNC1021 and UNC1215 potently antagonize L3MBTL3 binding to a H4K20me2 peptide (residues 17-25), and UNC1079 is a structurally similar but significantly less potent antagonist. Compounds screened at concentrations up to 30 μM. The IC_{50} values for UNC1021, UNC1215, and UNC1079 were calculated from 44, 17, and 6 replicate runs, respectively.

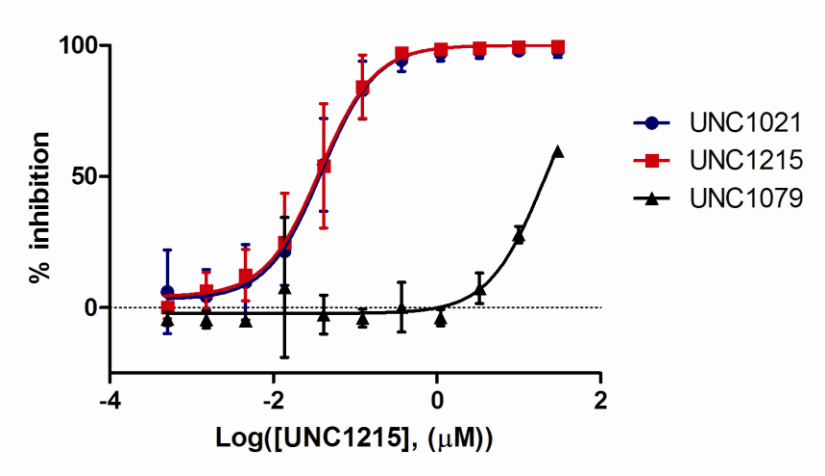

b) **Representative AlphaScreen binding curves for H4K20me and H4K20me2 peptides (residues 17-25) against L3MBTL3 (3MBT).** H4K20Me2 peptide binds L3MBTL3 more potently than the corresponding H4K20Me peptide. Both peptides bind weakly, similar to other interactions of this type.

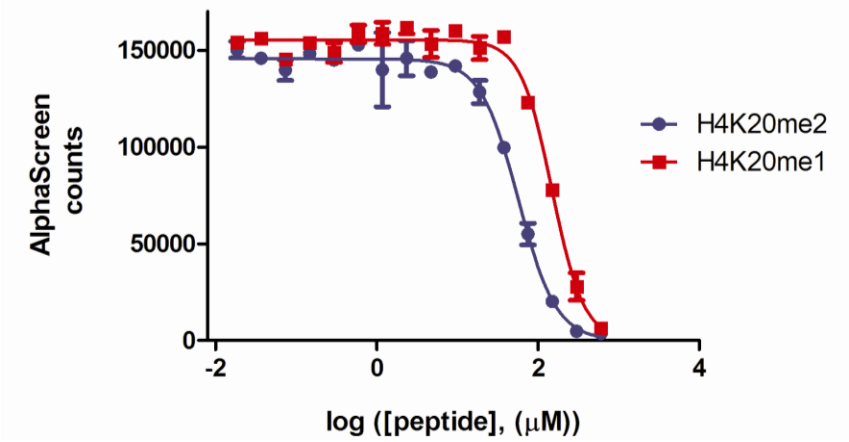

c) **Alphascreen binding curve for a methylated BCLAF1 peptide (residues 438-452 with K445me) against L3MBTL3 (3MBT).** The BCLAF Kme peptide (green) binds L3MBTL3 in this assay similarly to methylated H4K20 peptides.

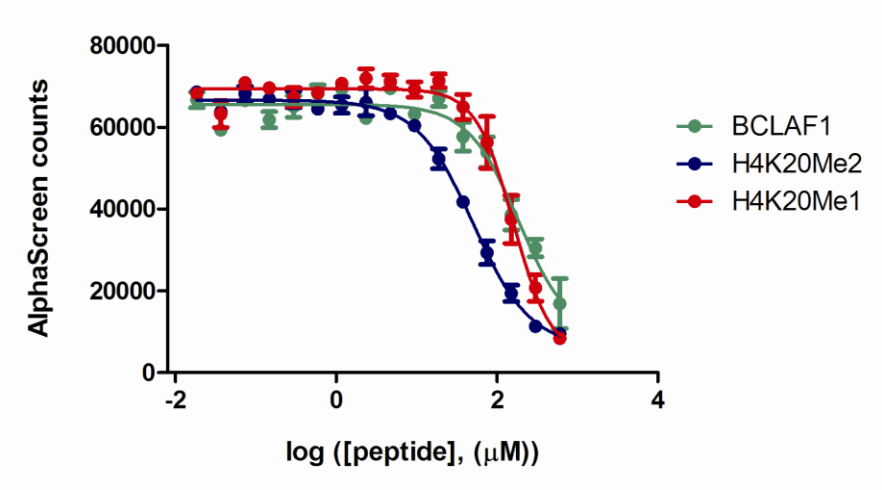

Supplementary Figure 2. Representative ITC binding curves.

a) UNC1079 is not a potent inhibitor of L3MBTL3. Representative ITC curve of inactive control compound, UNC1079, titrated into 3MBT WT, indicating little to no binding occurs under these conditions.

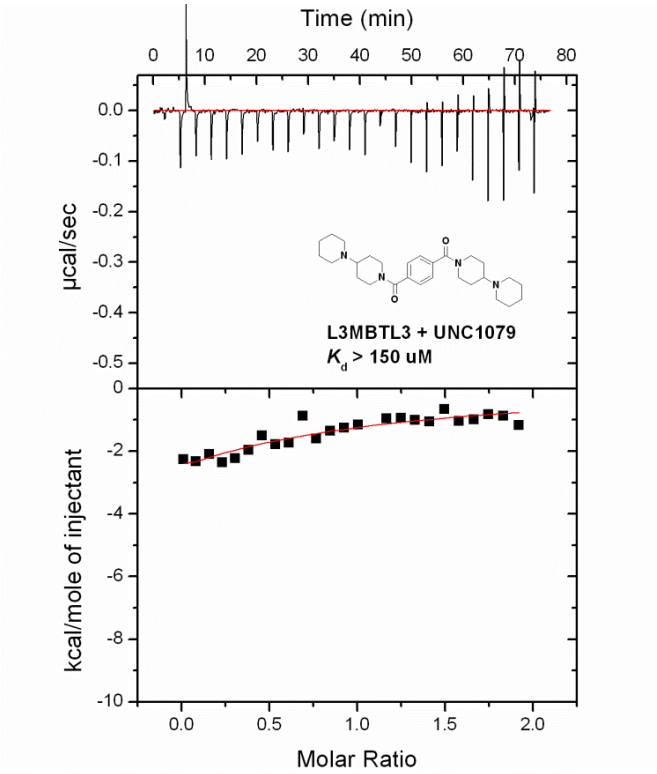

b) UNC1215 binding to L3MBTL3 F387A and L3MBTL3 H277A is reduced relative to wildtype.

Left: Representative ITC curve showing that mutagenesis of the domain 2 aromatic cage residue, F387, to alanine significant reduces binding to UNC1215 relative to wildtype. Right: Representative ITC curve showing that mutagenesis of H277 to alanine results in weakened binding to UNC1215 relative to wildtype.

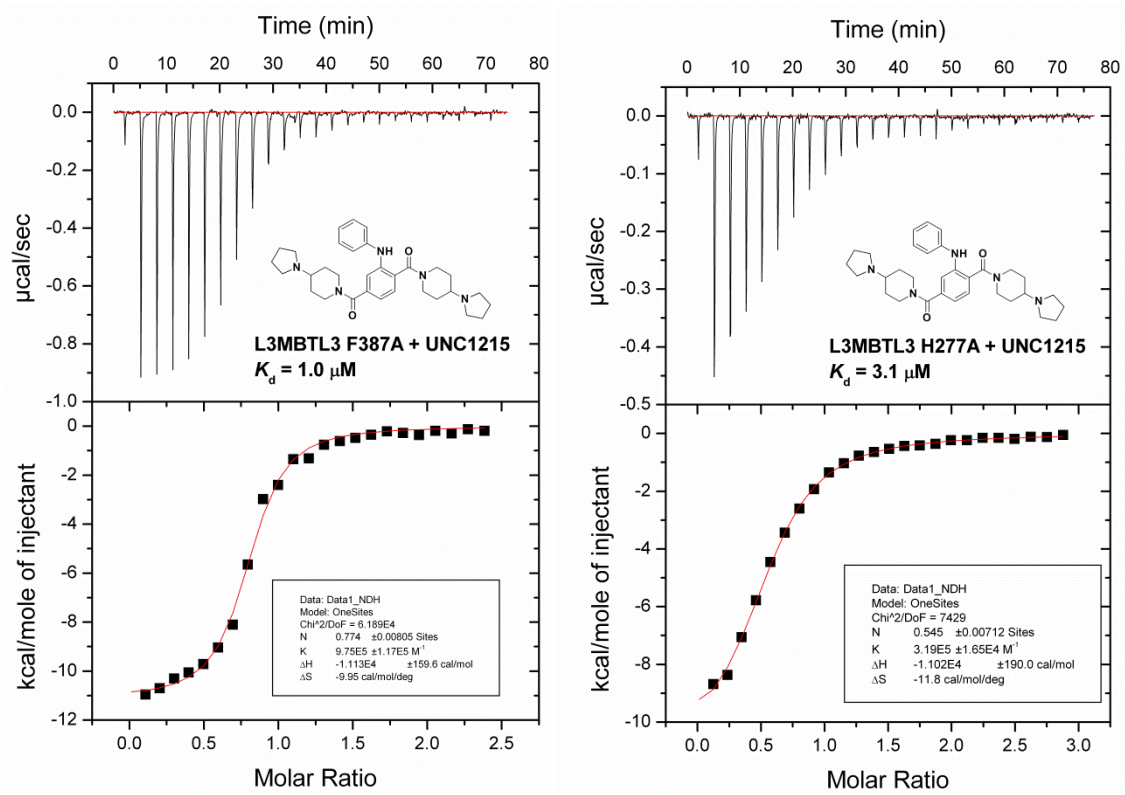

c) Biotin-UNC1215 binds L3MBTL3. Representative ITC curve of biotin-UNC1215 (**8**) titrated into 3MBT WT, indicating that the biotinylated analog binds almost as well as UNC1215.

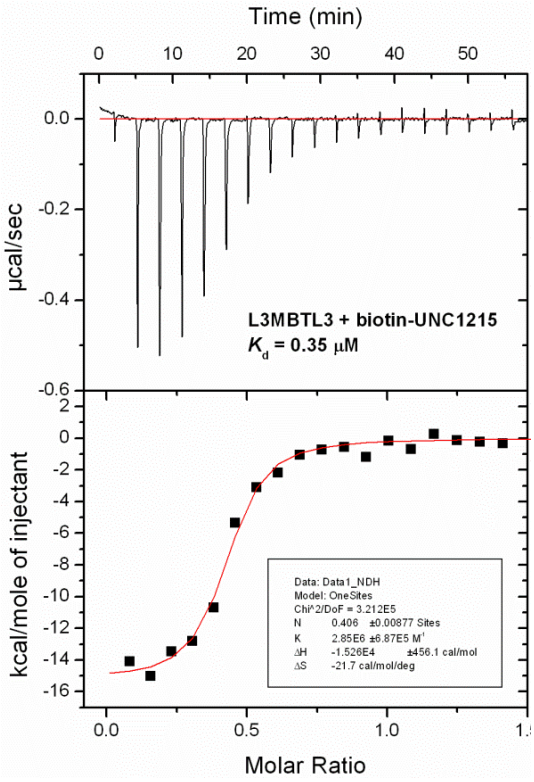

d) UNC1215 is selective for L3MBTL3 versus other Kme binding proteins. Representative ITC curves for UNC1215 binding to other Kme reader proteins that showed positive binding on the protein microarray, including L3MBTL1, 53BP1 Tudor, SFP30 (*S.p.*) Tudor, PHF20 Tudor, PHF20L1 Tudor, PHF20L1 MBT, and MRG15.

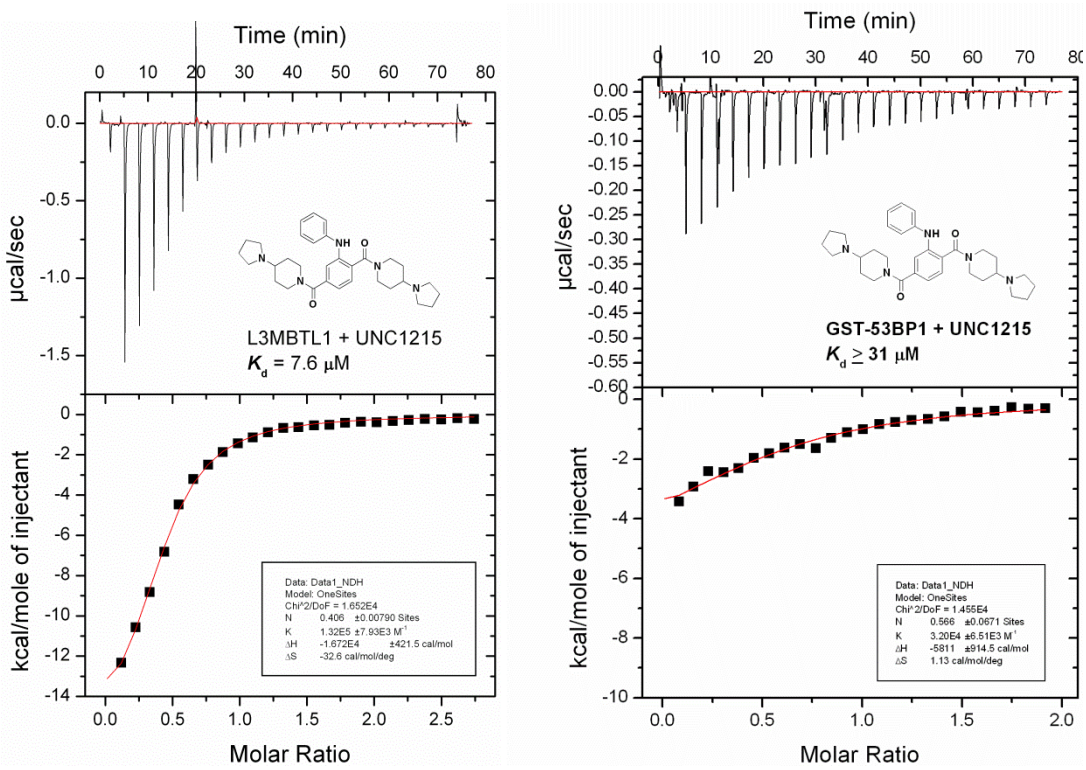

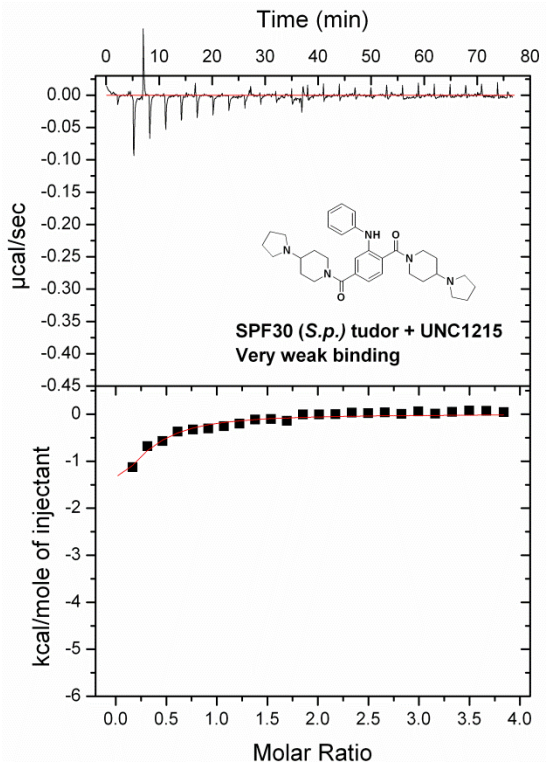
Time (min)
µcal/sec
kcal/mole of injectant
Molar Ratio
SPF30 (S.p.) tudor + UNC1215
Very weak binding

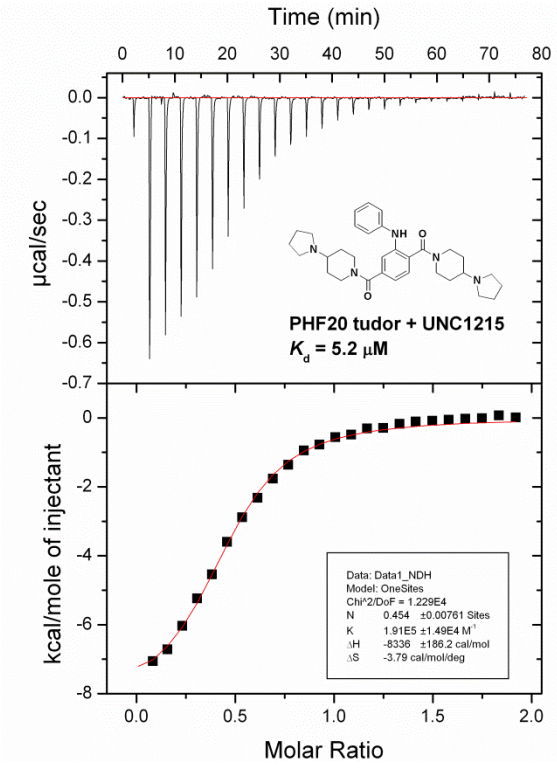
Time (min)
µcal/sec
kcal/mole of injectant
Molar Ratio
PHF20 tudor + UNC1215
K_d = 5.2 µM
Data: Data1_NDH
Model: OneSites
Chi^2/DoF = 1.229E4
N 0.454 ±0.00761 Sites
K 1.91E5 ±1.49E4 M-1
ΔH -8336 ±186.2 cal/mol
ΔS -3.79 cal/mol/deg

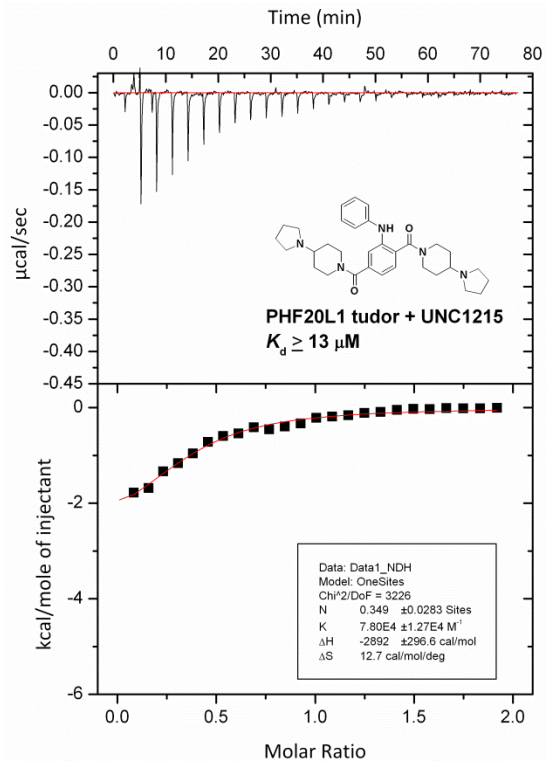
Time (min)
µcal/sec
kcal/mole of injectant
Molar Ratio
PHF20L1 tudor + UNC1215
$K_d \geq$ 13 µM
Data: Data1_NDH
Model: OneSites
Chi^2/DoF = 3226
N 0.349 ±0.0283 Sites
K 7.80E4 ±1.27E4 M-1
ΔH -2892 ±296.6 cal/mol
ΔS 12.7 cal/mol/deg

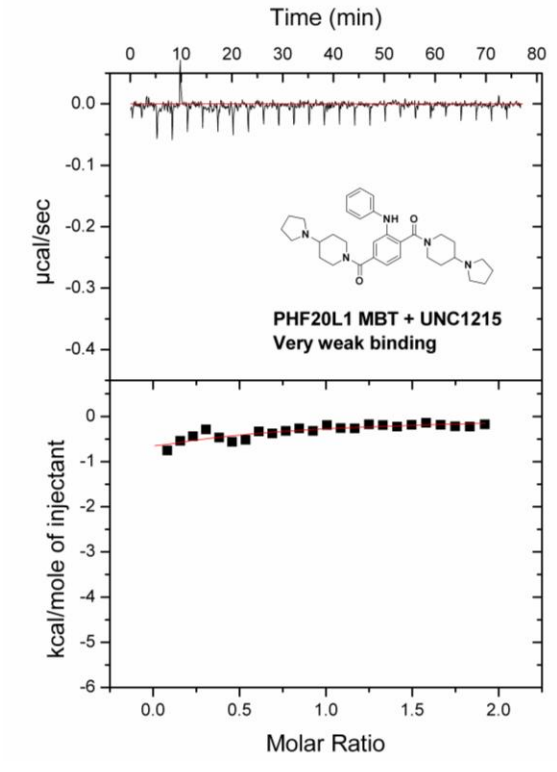
Time (min)
µcal/sec
kcal/mole of injectant
Molar Ratio
PHF20L1 MBT + UNC1215
Very weak binding

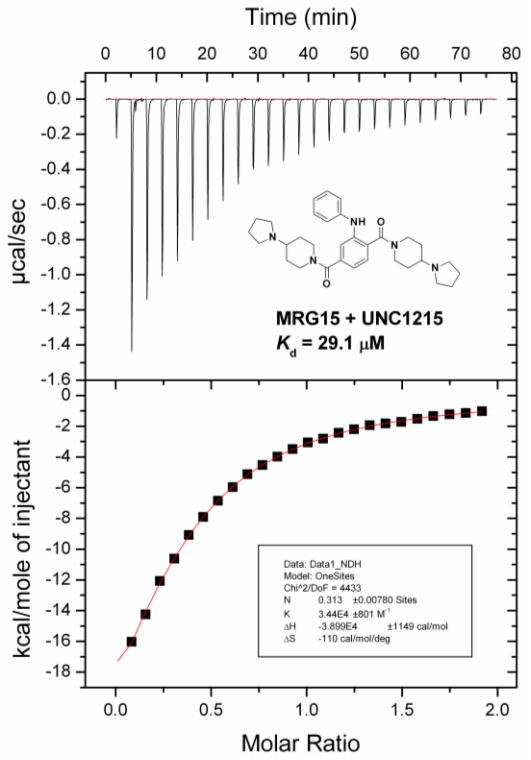

Supplementary Figure 3. UNC1215 induces L3MBTL3 dimerization in gel filtration experiments. The 3MBT monomer peak in the absence of UNC1215 is shown in pink (retention volume of 88.7 mL). Upon incubation with UNC1215, 3MBT forms a dimer, resulting in a higher molecular weight peak as shown in blue (retention volume of 96.9 mL).

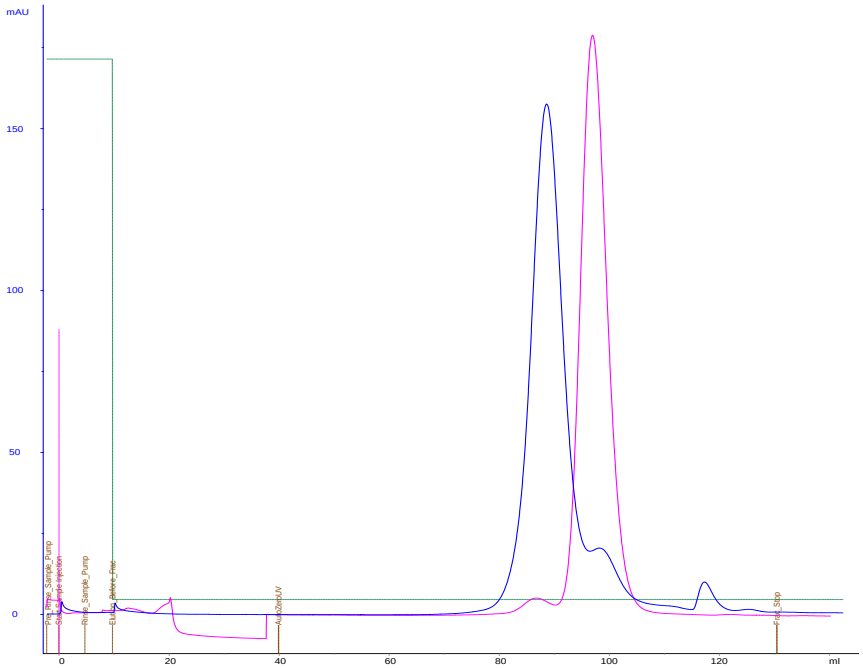

Supplementary Figure 4. UNC1215, H4K20me2, and H3K9me3 selectivity against the methyl-lysine and methyl-arginine reader domains.

a) A collection of 268 GST-fusion proteins consisting of methyl-lysine and methyl-arginine reader domains arrayed in duplicate on a nitrocellulose membrane. This library is composed of domains found in chromatin-associated proteins that were cloned as GST fusions, and has been previously described.[5,6] The slide was probed with biotin-UNC1215 followed by a fluorescent streptavidin conjugate to visualize binding interactions. Biotin-UNC1215 was found to positively interact with only a small number of proteins (circled in red), and with the exception of MRG15, each is a known H4K20me1/2 reader.

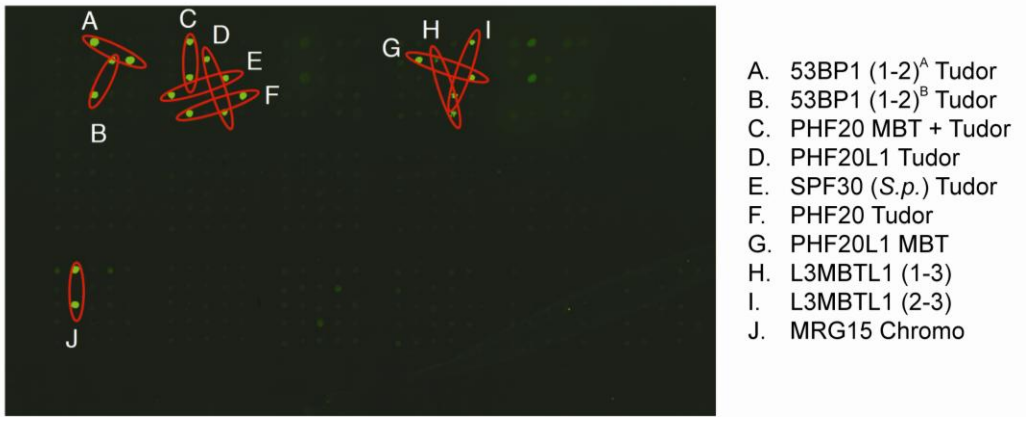

b) The two panels were probed with Cy3-labelled H3K9me3 and H4K20me2 peptides to identify distinct "readers" for each of these marks. The "readers" are listed on the side of the figure, with the domain type in brackets. Some proteins interact with the non-methylated control peptide and they are blocked in orange.

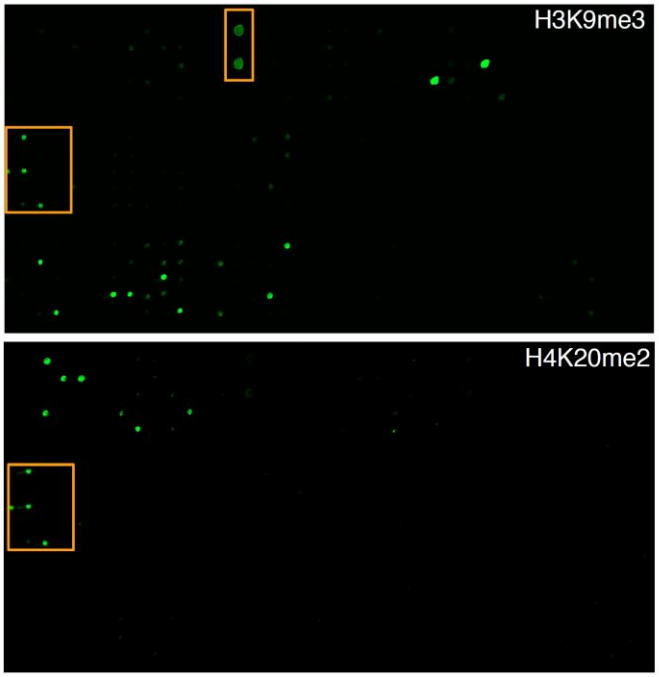

WDR5 (WD40)
MPP8 (Chromo)
HP1 beta (Chromo)
CDY1 (Chromo)
HP1 gamma (Chromo)
CDYL2 (Chromo)
Nonspecific interactions

53BP1(1-2)^{A} (Tudor)
53BP1(1-2)^{B} (Tudor)
SPF30 (*S.p.*) (Tudor)
PHF20(2) (Tudor)

c) A key to the CADOR array shown in panel a and b.

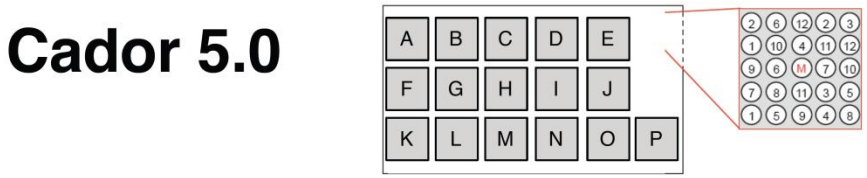

TUDOR A1 TDRD2(NP_006853) A2 TDRD3(Q9H7E2) A3 TDRD4-1(Q9NUY9) A4 TDRD4-2(Q9NUY9) A5 TDRD4-3(Q9NUY9) A6 TDRD7-1(NP_055105) A7 TDRD7-3(NP_055105) A8 EBNA-2Co-A(NP_055205) A9 Ret-bp1(AAB28543) A10 M96(AAH10013) A11 53BP1(1-2)(NP_005648) A12 53BP1(1-2)(NP_005648)	TUDOR + B1 2C(NP_055876) B2 RBP1 like-2 (NP_112739) B3 SMN (NP_075012) B4 PHF20L1(NP_057102) B5 PHF20(NP_057520) B6 PHF20 MBT+TDR(NP_057520) B7 Pombe 1(CAA22823) B8 JMJD2A-2(NP_055478) B9 JMJD2A1-2(NP_055478) B10 LBR TDR(NP_919424) B11 LBR211(NP_919424) B12 SPF30(c)(O75940)	TUDOR / Tudor-Like C1 Lin9 TDR(b)(AAH65302) C2 JMJN 2B WT(f)(NP_055830) C3 ARI4A (e)(NM_002892) C4 PHF19(NP_00100936) C5 SND1 (e)(NM_014390) C6 UHRF1 Tudor-like(a) C7 C420 Tudor-Like(p) C8 C460 Tudor-Like(p)	MBT D1 SFMBT F.L(j) D2 SFMBt 4xMBT(j) D3 L3MBTL1(2-3)(NP_056293) D4 L3MBTL1(1-3)(NP_056293) D5 SCMH1(AAH21252) D6 SCML1(NP_057413) D7 SCML2(AAH64617) D8 LML2(Q969R5) D9 PHF20 MBT(NP_057520) D10 PHF20L1 MBT(NP_057102)	His-MBTs / WD40 E1 SFMBT1(a) E2 SFMBT2(a) E3 L3MBTL1(a) E4 L3MBTL2(a) E5 L3MBTL3(a) E6 SCMH1(a) E7 WD40 -WDR5(d)(NP_543124) E8 WD40 -WDR9(NM_018963) E9 WD40 -RbAb46(d)(BT007309) E10 WD40 -RbAb48(d)(X74262) E11 WD40 -HIRA(CR456503) E12 WD40 -Mep50(d)(AF478464)	
PhD + F1 BPTF(P+B)(BAA89208) F2 ING2(e)(AAH50003) F3 PHF2(NP_005383) F4 PHF8(CAI42860) F5 DATF1(CAI95708) F6 Rag2(NM_000536) F7 PCCX1(NP_055408) F8 P300(P+B)(NM_001429) F9 PHF20 PHD(NP_057520) F10 PHD PHF3 F11 PHD PHF5 F12 PHD CHD5 (1-2)	PhD G1 Dnmt3a-His/GST(g) G2 Dnmt3b-His/GST(g) G3 DnMT3L N-term-His/GST(g) G4 Trim24 Brd-PhD(i) G5 ING3(e) (NP_061944) G6 ING4(e) (NP_001121054) G7 ING5(e) (NP_115705) G8 PHD _TIF1A(e) (O15164) G9 TRI66(e) (O15016) G10 BRPF1(e) (P55201) G11 MLL4(e) (Q9UMN6) G12 MTF2(e) (Q9Y483)	PhD + H1 JMJD2APhD+2Tudor(NP_055478) H2 JMJCPhD(NP_055478) H3 M96Tudor+PhD(AAH10013) H4 MYST4PhD+PhD(AAH48199) H5 NSD1PhD+PWWP(Q96L73) H6 WHSC1PhD+PWWP(NP_579877) H7 BS69PhD+ BRD(AAH12586) H8 ATRX H9 RAL1 H10 BAZ1b/WSTF H11 CBP H12 TAF3 (k)	BROMO I1 GCN5(Q92830) I2 TAF1- D1(NP_620278) I3 TAF1- D2(NP_620278) I4 P/CAF (S71788) I5 SNF2 beta(S45252) I6 BAF180 1-2(NP_060635) I7 BAF180-3(NP_060635) I8 BAF180 3-4(NP_060635) I9 BAF180 5-6(NP_060635) I10 KAP-1(AAB37341) I11 P300(NP_004371) I12 WDR9 2(Q9NSI6)	BROMO /SANT / TSN J1 Bromo-BAZ(NP_075381) J2 Bromo-BRDT 1(AAH62700) J3 SANT-MPP11-like(XP_379909) J4 SANT-N-CoR2-2(Q9Y618) J5 SANT-RERE(AAH62342) J6 SANT-ADA2(NP_001479) J7 SANT-Zuotin Rel.(XP_168590) J8 TSN-p100(o) (NP_055205) J9 TSN-p100 m5(o) (NP_055205) J10 TSN-p100 m6(o) (NP_055205)	
CHROMO K1 TIP60(h)(AAB18236) K2 CHD2(h)(AAB87382) K3 CHD4(h)(AAH38596) K4 MPP8(h) (NP_059990) K5 SMARCC2(h)(AAH26222) K6 MRG15(h)(AAD29872) K7 RBBP1(h)(AAD41239) K8 PC2(h)(AAB80718) K9 PC3(h)(AAG09180) K10 CHD5(h)(AAK56405) K11 CHD7 (1-2)(AB037837) K12 CBX6/NPCD(BC012111)	CHROMO L1 MI-2(h)(CAA60384) L2 HP1alpha(h)(P45973) L3 HP1gamma(h)(NP_057671) L4 MSL3-like(h)(AAD38499) L5 SUV39H1(h)(AAB92224) L6 CBX1/HP1beta(h)(AAD21972) L7 HP1 beta(h)(P23197) L8 CDY1(h)(AAD22735) L9 CHD1(e) (NP_001261) L10 CBX4/PC2(e) (NM_003655) L11 CBX7/RP4(e) (NM_175709) L12 CBX5/HP1alpha(e)NM_012117)	CHROMO / BRK /MRG M1 CBX3/HP1gamma(e)(NM_016587) M2 CBX2/CDCA6(e) (NM_005189) M3 CDYL2(e) (NM_152342) M4 CBX8/PC3(e) (NM_020649) M5 BRK_SMCA2 (e)(NM_003070) M6 BRK_SMCA4(e) (NM_003072) M7 BRK_CHD6(e) (NM_032221) M8 BRK_CHD7 (e)(NM_017780) M9 BRK_Q6DTK9 (e)(NM_025134) M10 MRG_MSL3v1(e) (NM_078629) M11 MRG15(e) (NM_206839)	PWWP N1 BRPF1(AAH53851) N2 DNMT3B(Q9UBC3) N3 HDGF (P51858) N4 HRP-3(BAA90477) N5 MSH6(P52701) N6 NSD1(Q96L73) N7 WHSC1-1(NP_579877) N8 PSIP1(e) (NM_033222 N9 BRD1(e) (NM_014577 N10 ZCPW1 (e)(AL136735 N11 MBD5 (e)(NM_018328	PWWP / CW / SWIRM O1 PWWP_PKCB1(e) (NM_183047 O2 PWWP_HDGR3(e) (NM_016073) O3 PWWP_DNM3A (e) (NM_175629) O4 CW3(AAH02725) O5 CW5(BAA09485) O6 CW6(XP_087384) O7 SWIRM_ KIAA1915(BAB67808) O8 SWIRM_KIAA0601(CAB72299) O9 SWIRM_ADA2(NP_001479)	ANK Q1 ANK-BARD1 (NP_000456) Q2 ANK-GLP(m) (AAM09024.1) Q3 ANK-Notch (NP_060087) Q4 ANK-IKB alpha F.L. (e) Other Q5 TULP1 Q6 MeCP2(i) Q7 PHD_ ZFP-1 His/GST(n)

Supplementary Figure 5. Protein pulldown experiments with biotin-UNC1215 demonstrate binding to L3MBTL3 and other readers.

a) Biotin-UNC1215 pulls down GST fusions of MBT domain containing proteins L3MBTL1 and L3MBTL3, and the tudor domains of 53BP1.

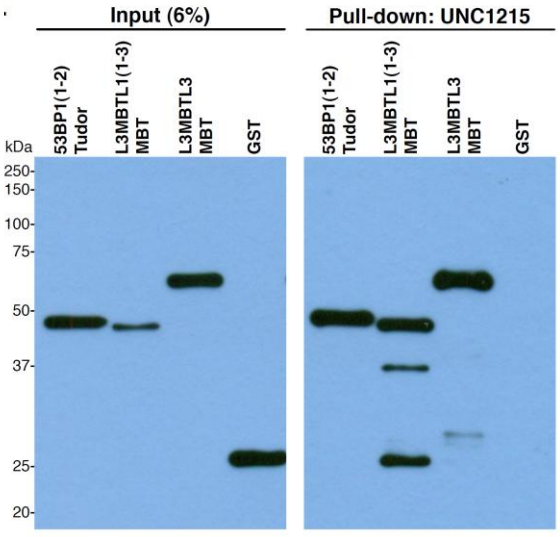

b) UNC1215 can pulldown GST fusion harboring the Tudor domains of 53BP1 (strongly), PHF20 (strongly) and SPF30^{sp} (weakly), but not the chromo domain of HP1. Interestingly, UNC1215 seems to induce dimerization of PHF20 tudors in this pull-down assay.

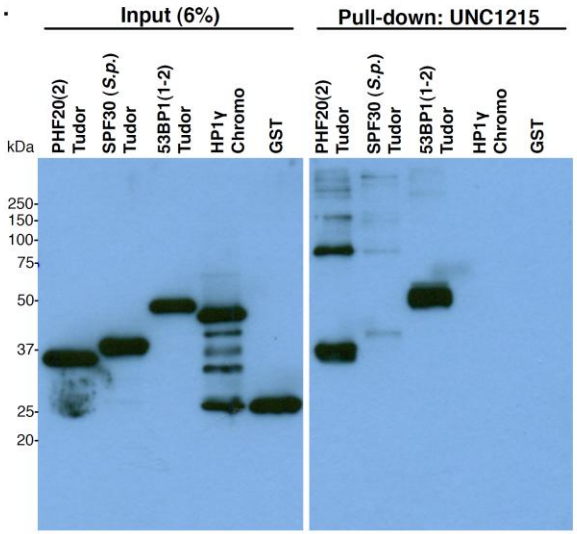

c) UNC1215 does not pulldown or bind the BAH domain of ORC1.

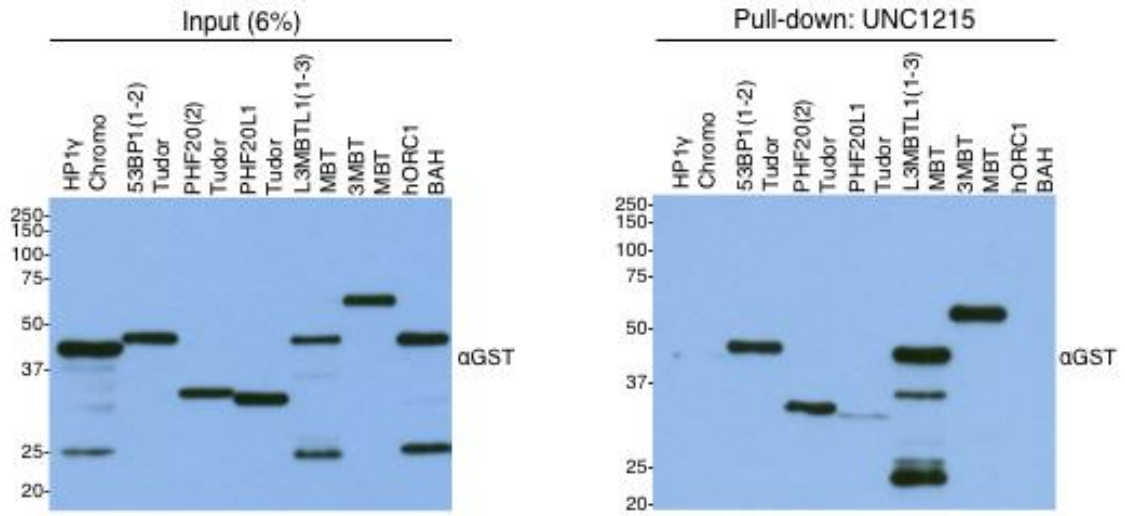

d) Original western blot from Figure 3b.

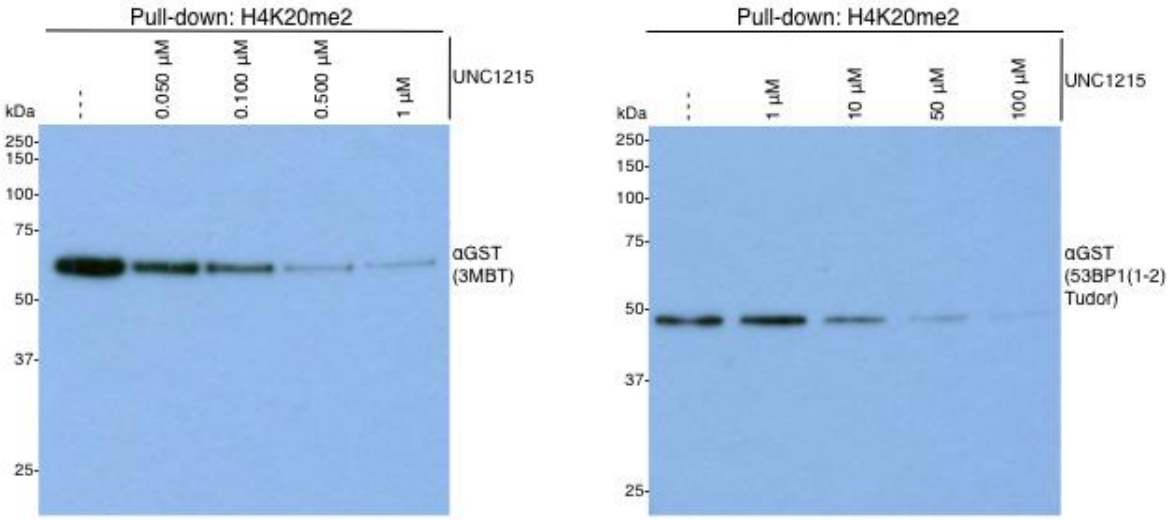

Supplementary Figure 6. UNC1215 is inactive against a panel of histone methyltransferases. The methyltransferase inhibition is evaluated by monitoring the transfer of a radioactive methyl group from SAM to lysine or arginine.

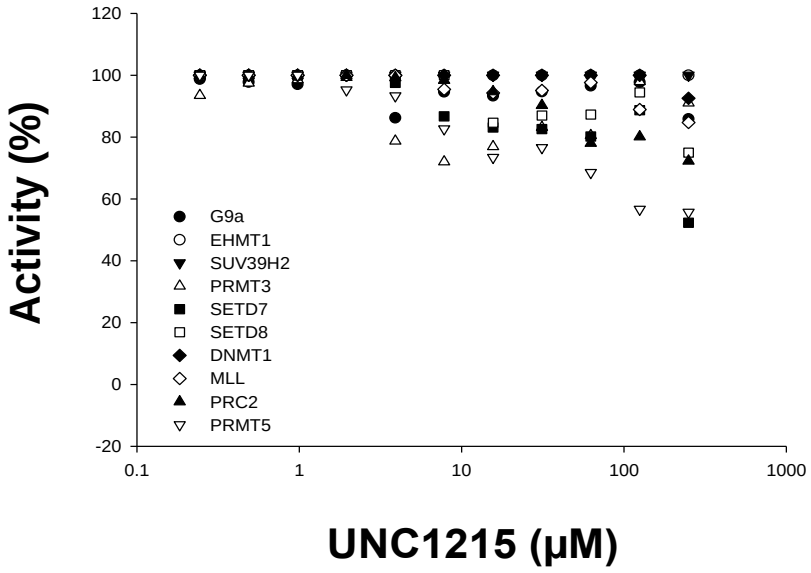

Supplementary Figure 7. M_1 and M_2 functional assays. UNC1215 had no agonist activity and weak functional antagonist activity at M_1 and M_2. The antagonist activity of UNC1215 was measured against 10 nM acetylcholine (hM_1) or 100 nM acetylcholine (hM_2). Atropine serves as an antagonist control.

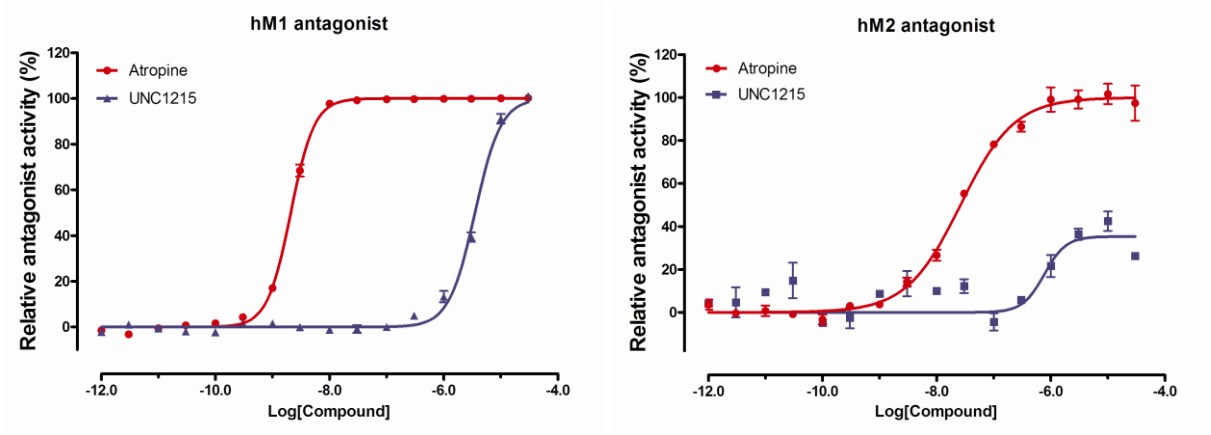

Supplementary Figure 8. Schild analysis at hM_1 and hM_2. Acetylcholine dose-responses were determined in the absence and presence of a graded concentration of UNC1215. Results were normalized and analyzed using a modified Lew-Angus method with GraphPad Prism 5.0.

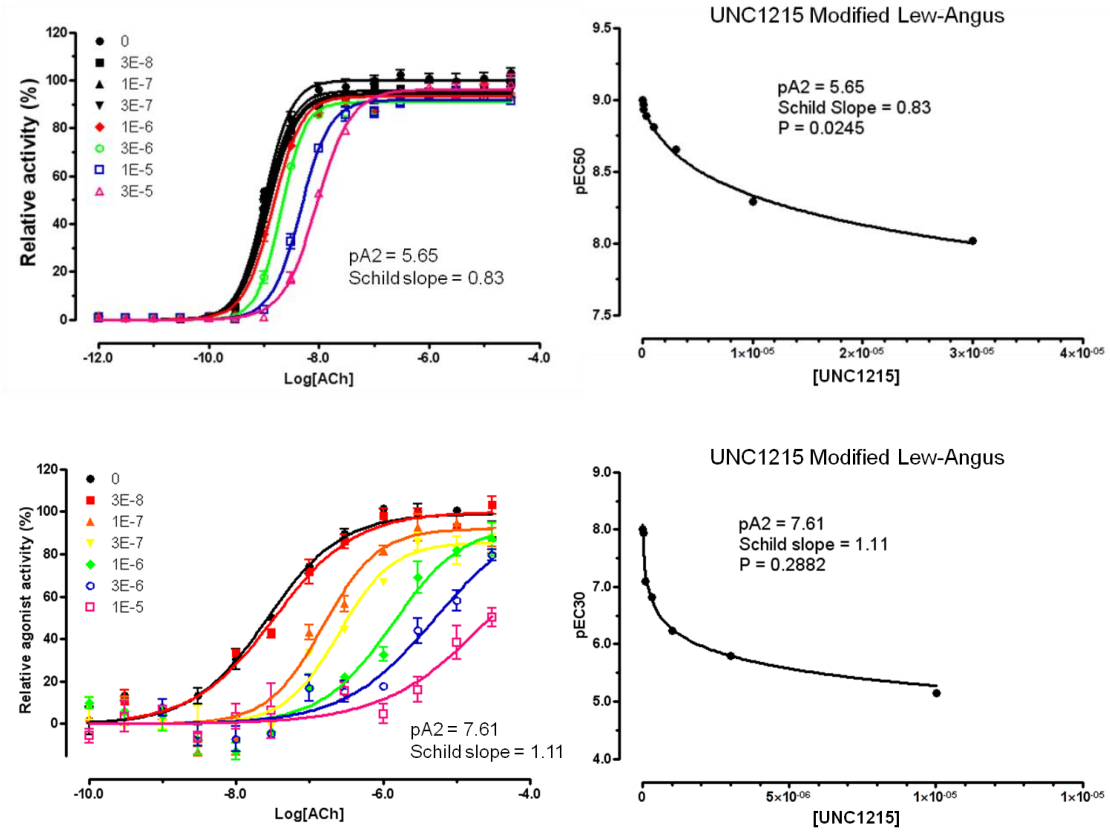

Supplementary Figure 9. CellTiter-Glo Luminescent Cell Viability Assay. UNC1215, UNC1021, and UNC1079 show no toxicity up to 100 µM.

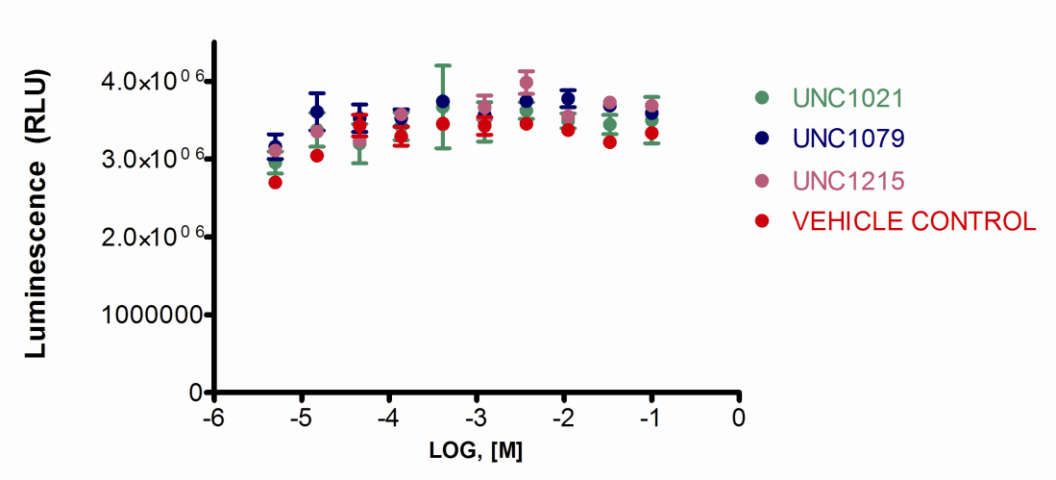

Supplementary Figure 10. FRAP results for GFP-3MBT D381A and GFP-3MBT D274A. FRAP results show that both domain 1 (D274A) and domain 2 (D381A) GFP-3MBT mutants show higher mobility than wildtype 3MBT.

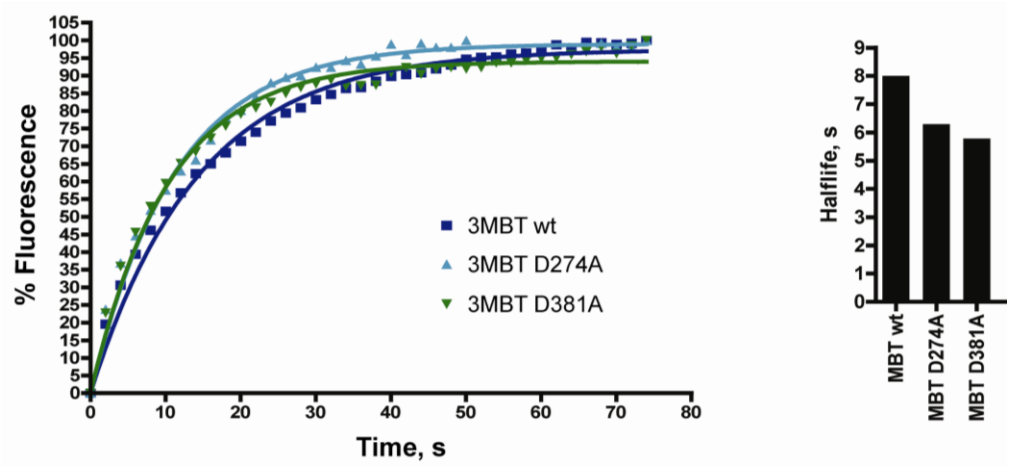

Supplementary Figure 11. N-terminal GFP-tagged FLMBT forms nuclear foci while N-terminal mCherry-tagged and C-terminal GFP-tagged FLMBT constructs do not form nuclear foci. N- and C-terminal 3MBT constructs form nuclear foci while N-terminal mCherry-tagged 3MBT does not. Scale bar, 10 µM.

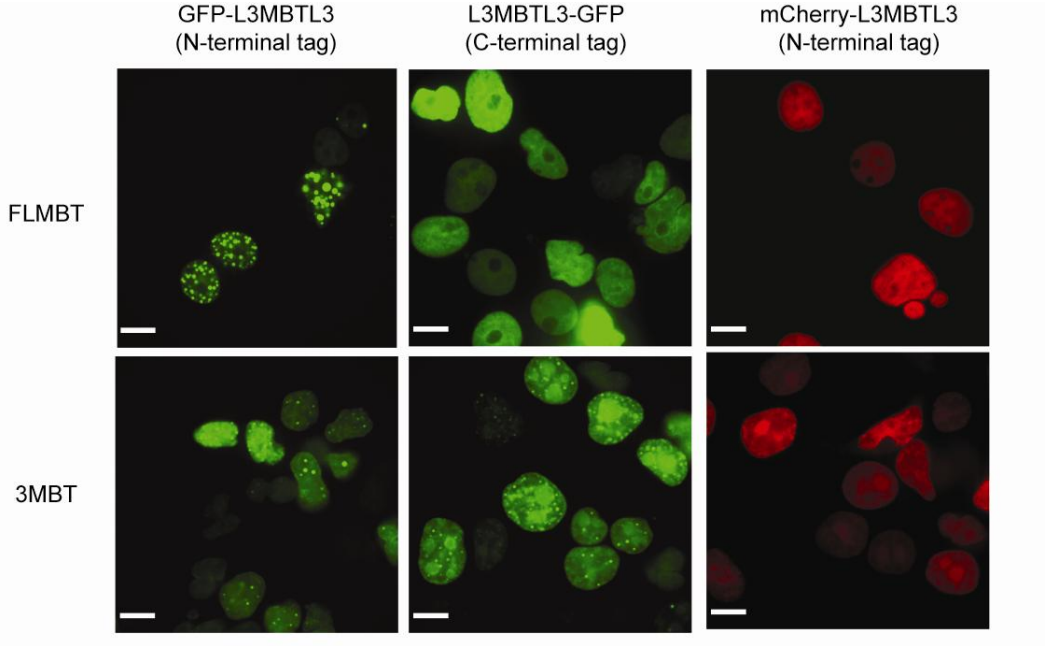

Supplementary Figure 12. UNC1215 inhibits GFP-3MBT foci formation. GFP fusions of 3MBT localize to the nucleus in HEK293 cells and UNC1215 inhibits the foci formation of GFP-3MBT in a dose response fashion, resulting in an IC_{50} of approximately 500 nM.

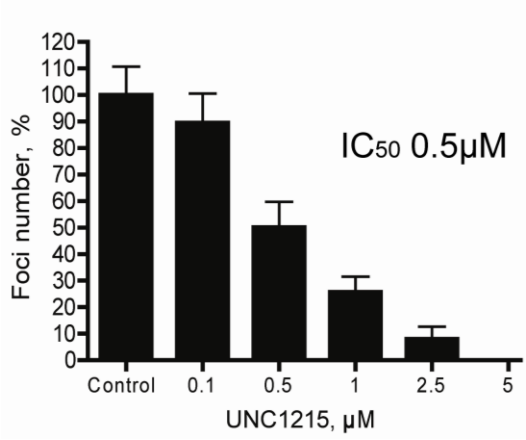

Supplementary Figure 13. GFP-3MBT and GFP-FLMBT nuclear localization and foci formation. In the case of GFP-3MBT, the domain 2 D381A mutant showed almost no foci formation and the domain 1 D274A mutant showed a reduction of foci formation by about 50 percent (293 cells were transfected with GFP fusion proteins; green is GFP and blue is Hoechst33342 stain; scale bar is 10 μm). For GFP-FLMBT, no change in the foci formation is observed for either mutant.

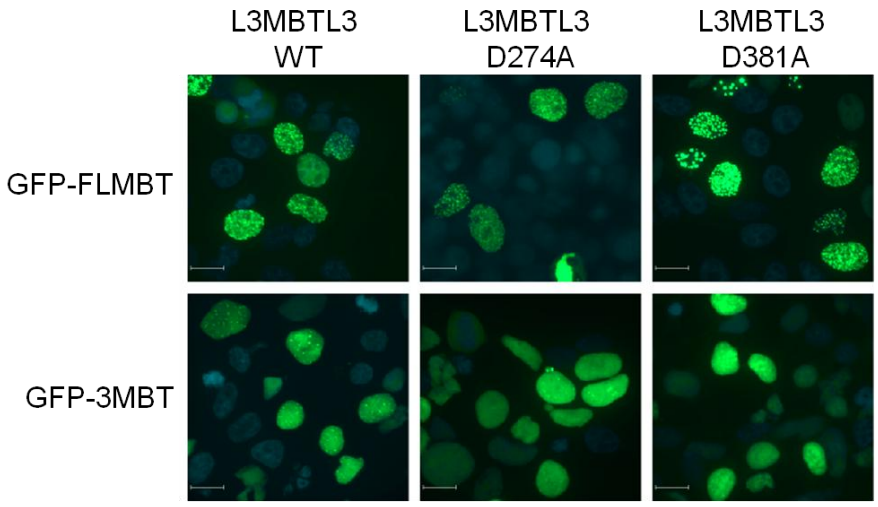

Supplementary Figure 14. GFP-FLMBTΔSAM nuclear localization. GFP-FLMBTΔSAM does not form nuclear foci and is homogeneously distributed throughout the nucleus in HEK293 cells.

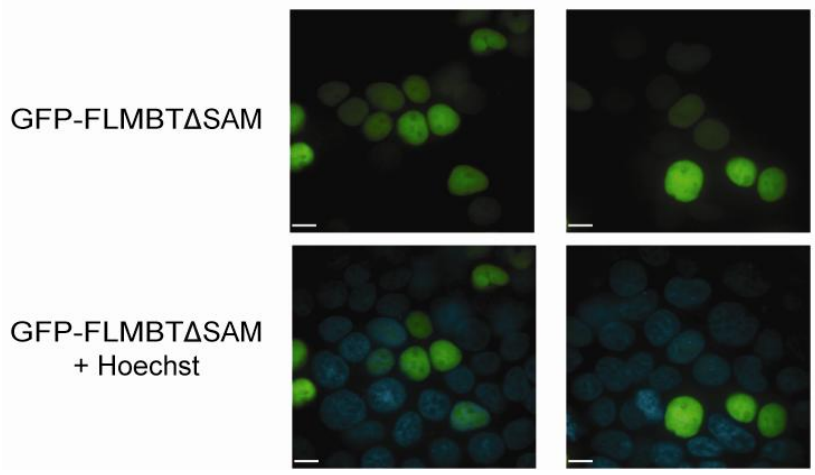

Supplementary Figure 15. Cellular localization of a fluorescent mero76-UNC1215 conjugate.

a) GFP-FLMBT WT. The merocyanine dye alone (mero76) shows no foci formation in the presence of GFP-FLMBT WT.

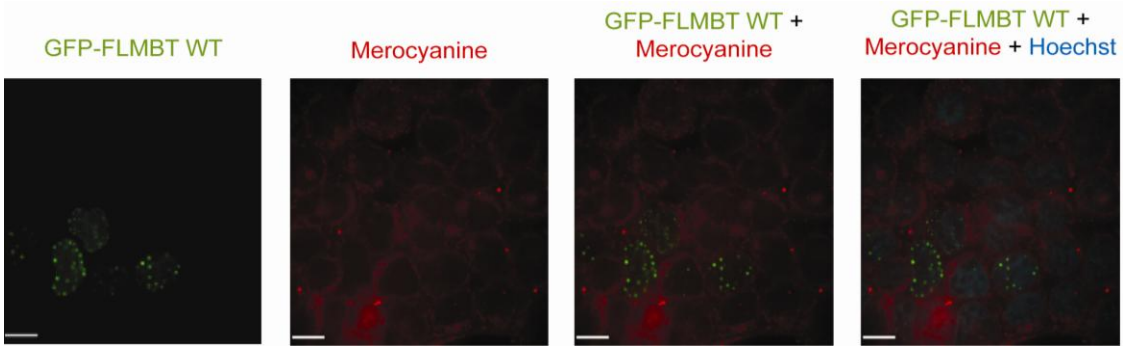

b) GFP-FLMBT D381A mutant. The mero76-UNC1215 conjugate shows no foci formation in the presence of GFP-FLMBT D381A (top row) or the mero76 dye alone (bottom row).

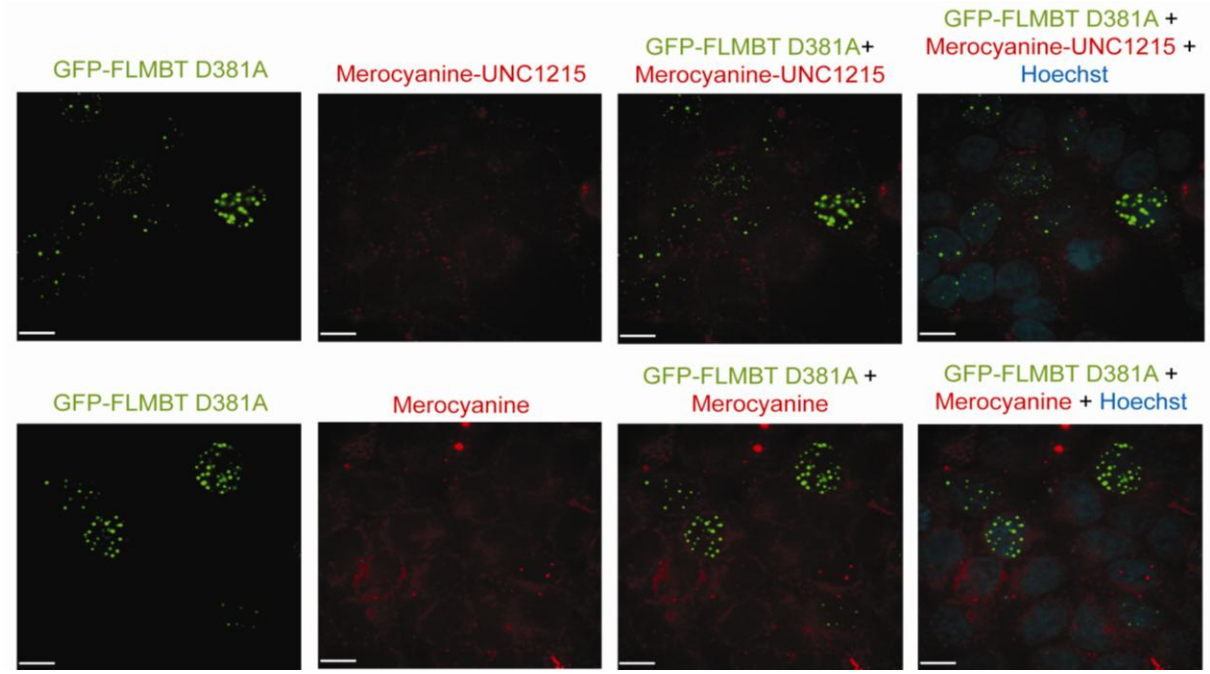

c) GFP-FLMBT D274A mutant. The mero76-UNC1215 conjugate forms foci and co-localizes with GFP-FLMBT D274A (top row), but the merocyanine dye alone does not (bottom row).

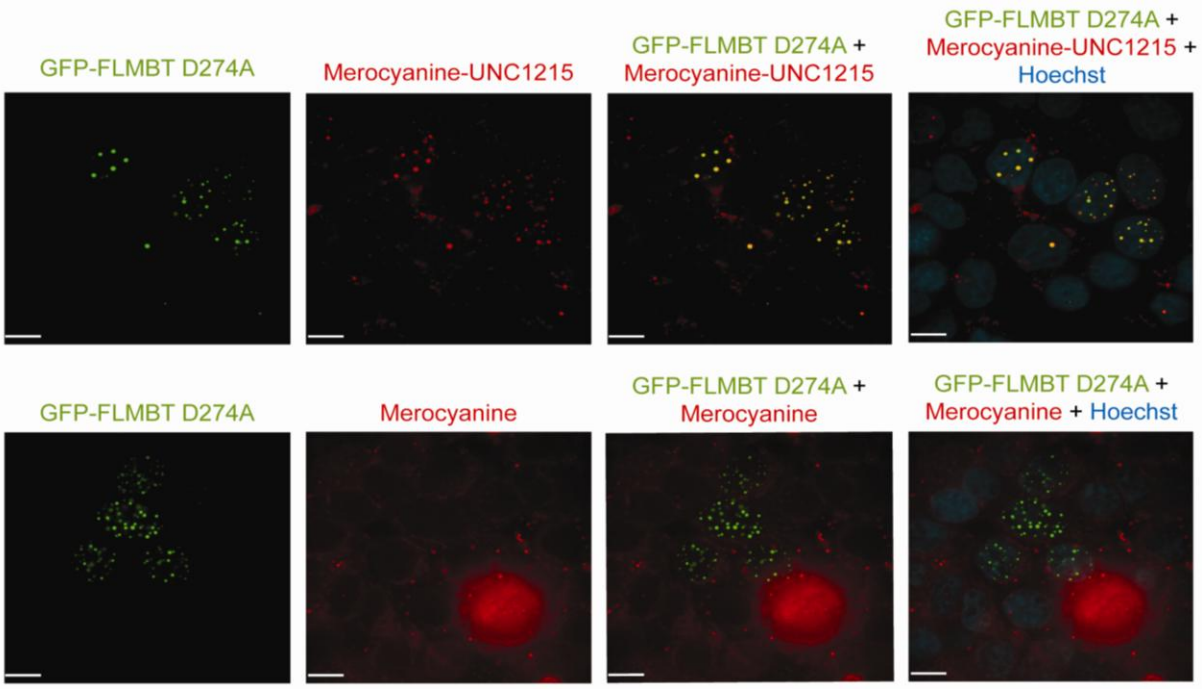

Supplementary Figure 16. FRAP results for GFP-FLMBT.

a) An increase in mobility of wildtype GFP-FLMBT was observed in the presence of UNC1215 by FRAP.

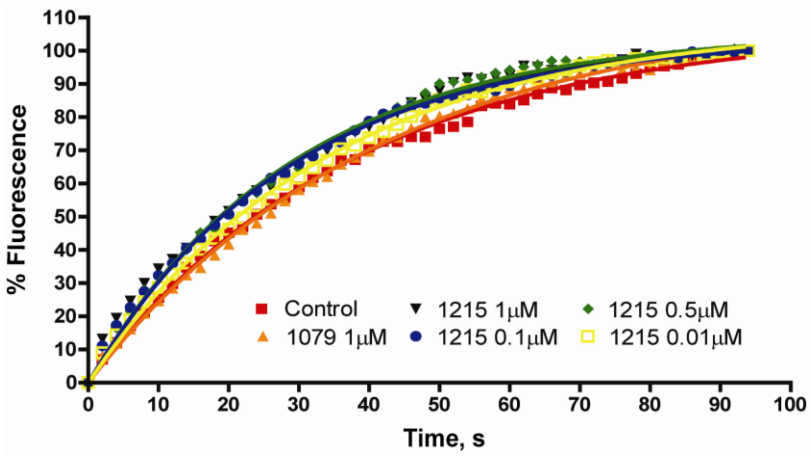

b) Domain 1 D274A mutant and domain 2 D381A mutant of GFP-FLMBT show higher mobility than wildtype FLMBT by FRAP.

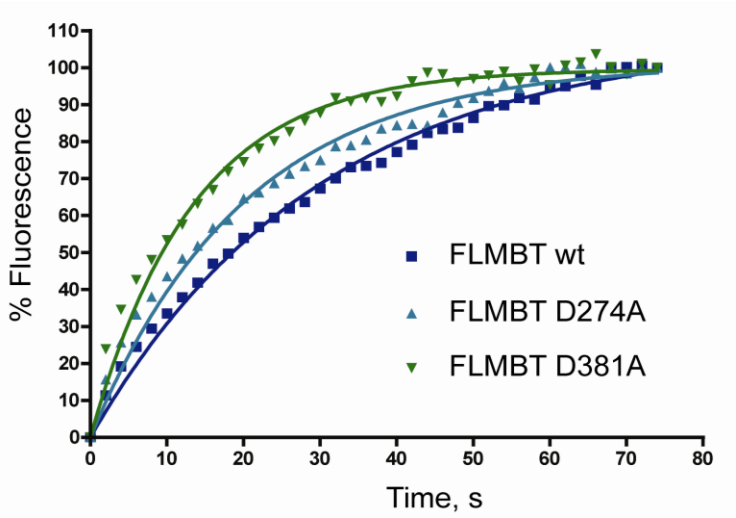

Supplementary Figure 17. Original western blot from Figure 5b. FLMBT binds to biotin-UNC1215 (5 nmol). The presence of increasing concentrations (1 or 10 equivalents relative to biotin-UNC1215) of untagged UNC1215 results in a decreased amount of bound FLMBT.

Supplementary Figure 18. L3MBTL3 binds BCLAF1. Immunofluorescence of L3MBTL3 and BCLAF1 in U2OS control and UNC1215 treated cells (green is L3MTL3, red is BCLAF1, and blue DAPI). GFP-3MBT strongly co-localizes with BCLAF1 and GFP-FLMBT showed weaker co-localization.

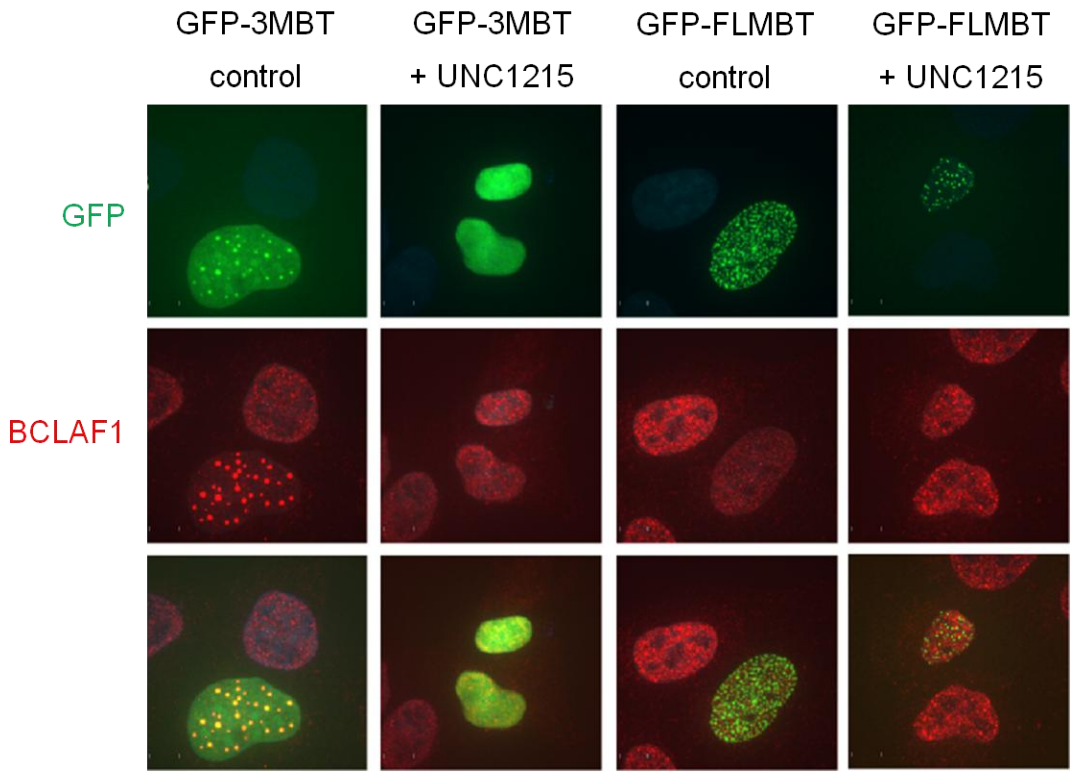

Supplementary Figure 19. Co-immunoprecipitation experiments with full length L3MBTL3 and BCLAF1.

a) Treatment with UNC1215 (1 μM) reduces the interaction between FLMBT and BCLAF1, whereas treatment with UNC1079 shows no effect. Similarly, the interaction between BCLAF1 and domain 2 mutant D381A is reduced relative to wildtype. U denotes untransfected cells.

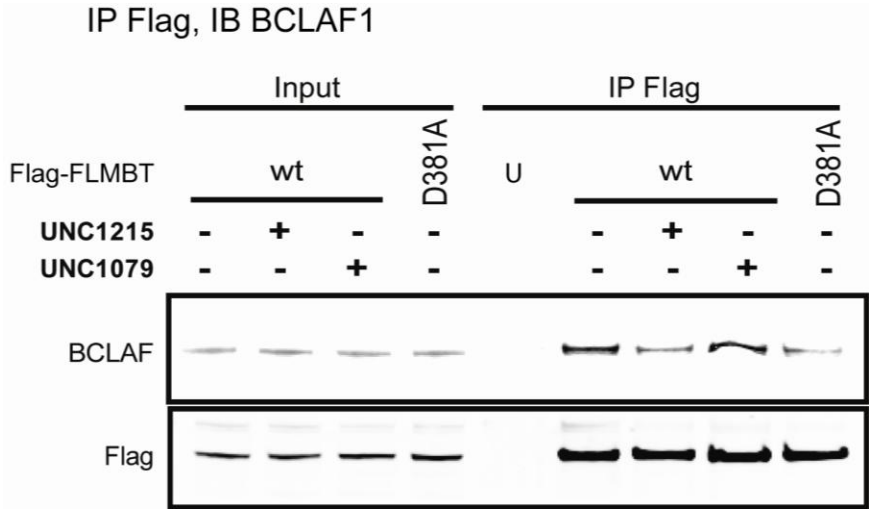

b) Original western blot from Figure 6b. The antibody signal is shown in green.

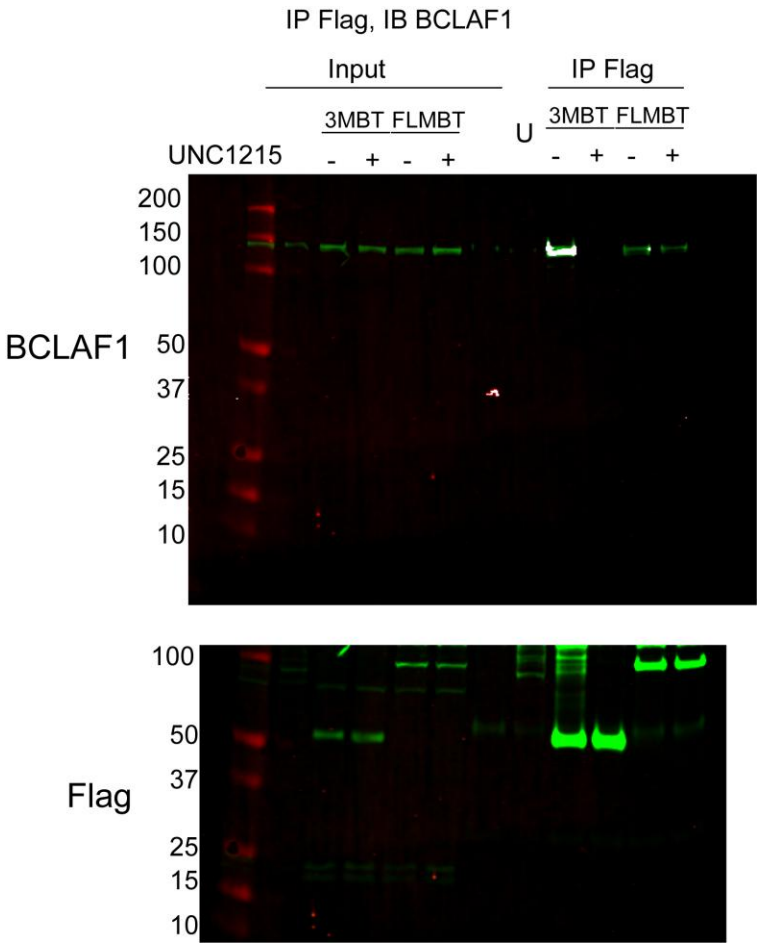

Supplementary Figure 20. GFP-3MBT co-immunoprecipitates with flag-3MBT in the absence and presence of UNC1215. HEK293 cells were transfected with flag-3MBT, GFP-3MBT, or both, and treated with UNC1215 (2 μM) or water as a control, followed by immunoprecipitation with an anti-flag antibody (or an anti-IgG antibody as a negative control). Both flag-3MBT and GFP-3MBT were detected with and without UNC1215 treatment, providing evidence for 3MBT dimerization in cells. This result supports the notion that the MBT domains may have a tendency to dimerize *in vivo*.

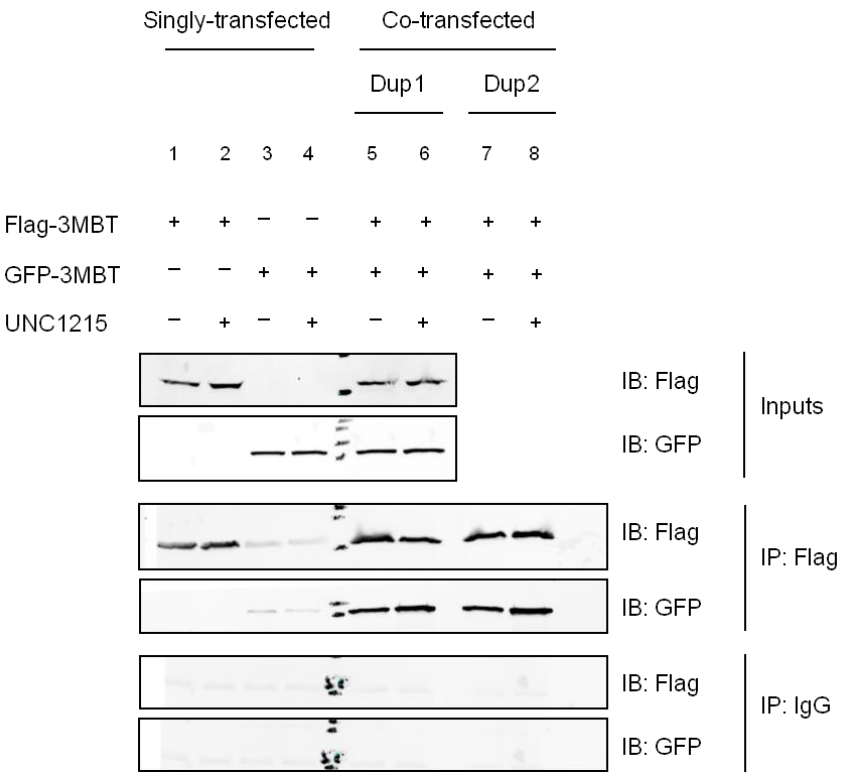

Supplementary Figure 21. Domain architecture of the L3MBTL3 constructs.

a) 3MBT constructs. Schematic of truncated 3MBT construct and tagged fusion proteins.

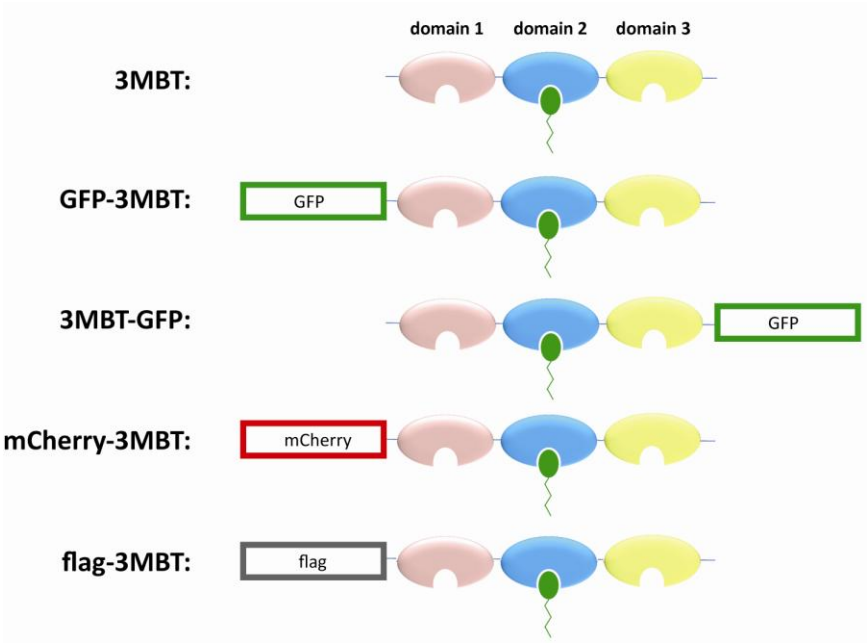

b) Full length L3MBTL3 constructs. Schematic of FLMBT construct and tagged fusion proteins.

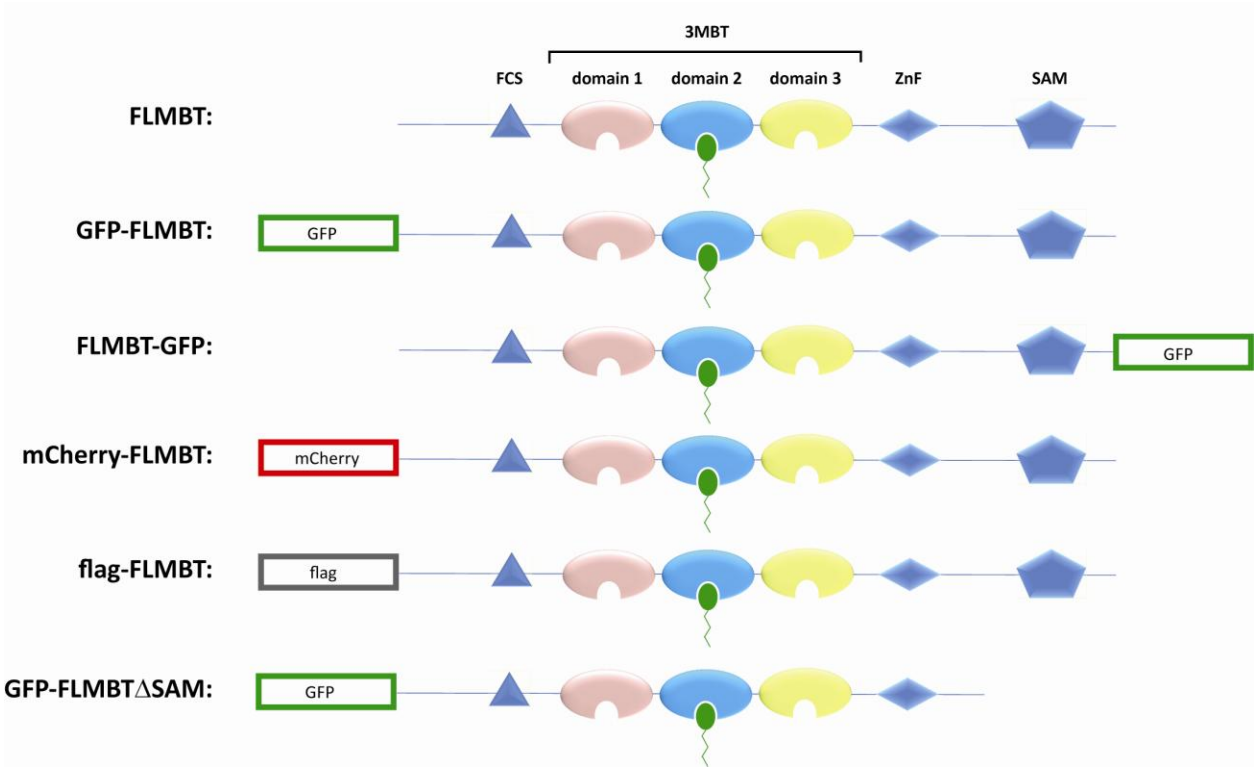

Supplementary Figure 22. ^{1}H NMR spectrum of UNC1215 (1) as a TFA salt. Signal broadening is observed, particularly when the compound exists as a TFA salt, due to slow rotation of the amide bonds on the NMR timescale.

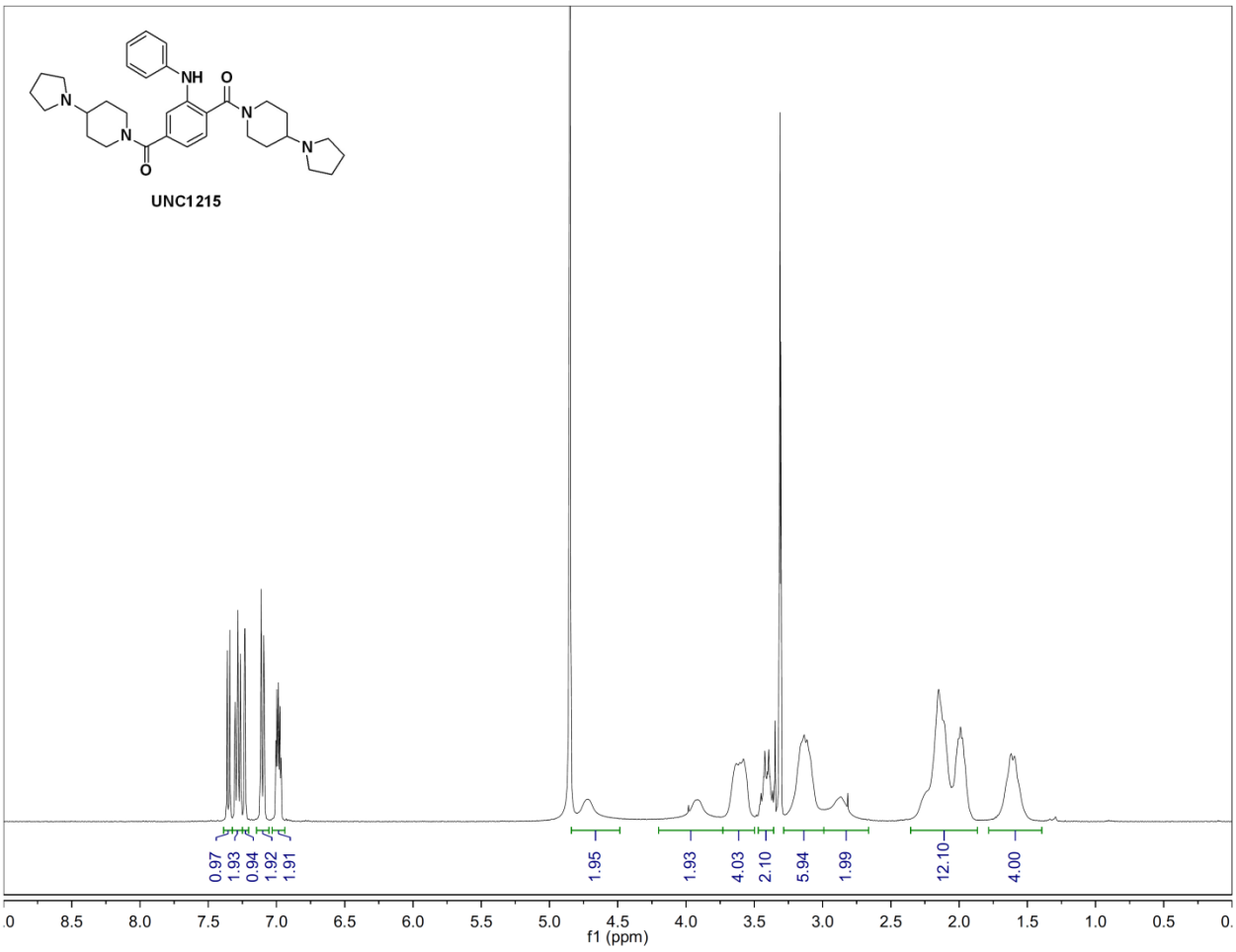

Supplementary Figure 23. ^{13}C NMR spectrum of UNC1215 (1) as a TFA salt.

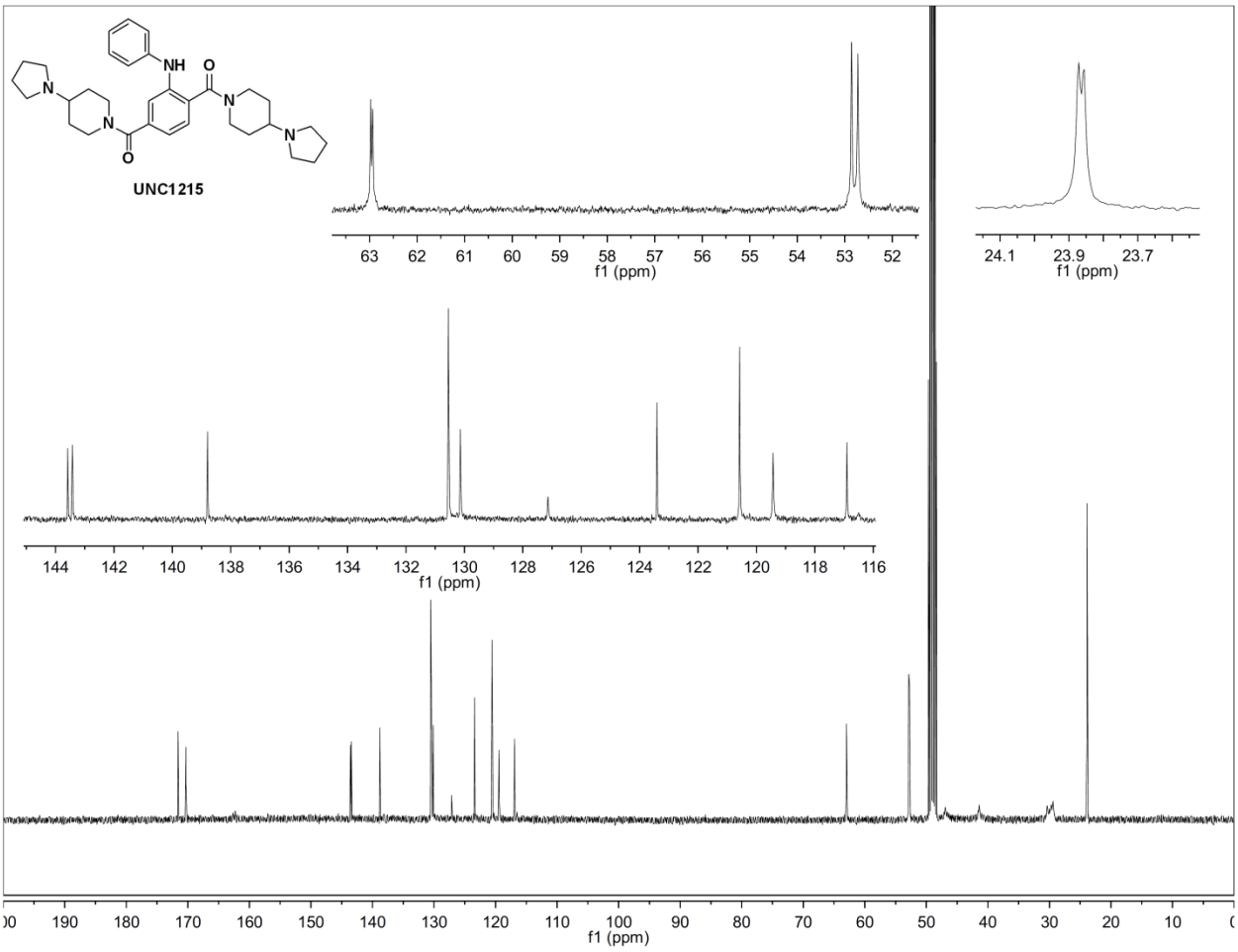

Supplementary Figure 24. LCMS trace of UNC1215 (1) at 220 and 254 nm.

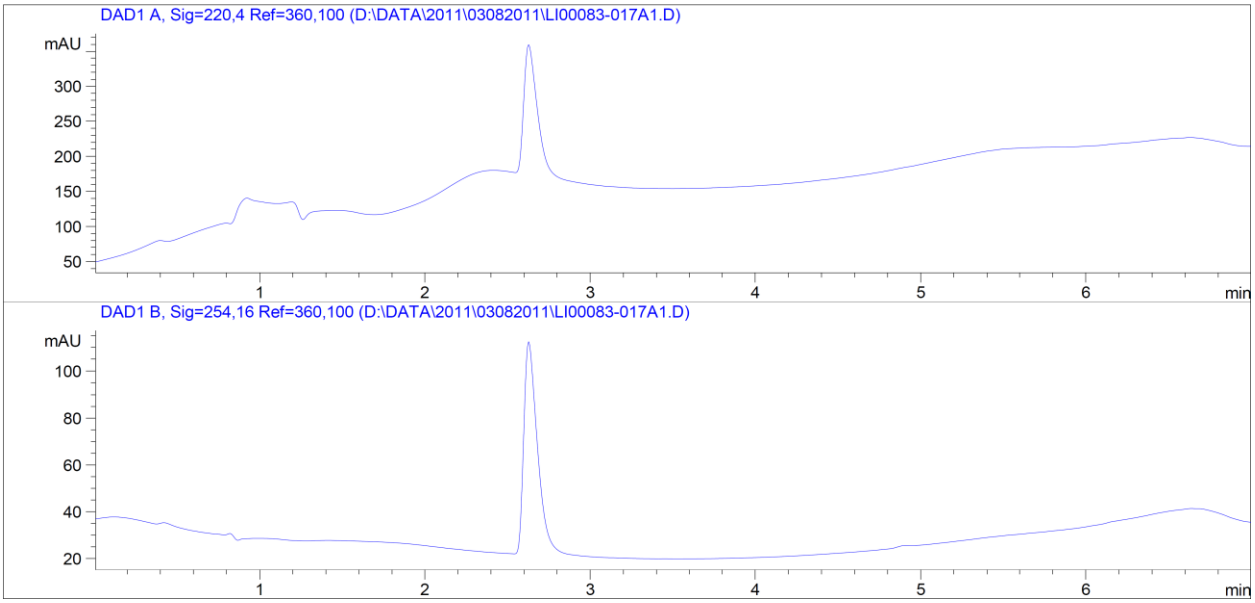

Supplementary Figure 25. ^{1}H NMR spectrum of UNC1021 (2) as a TFA salt. Signal broadening is observed, particularly when the compound exists as a TFA salt, due to slow rotation of the amide bonds on the NMR timescale.

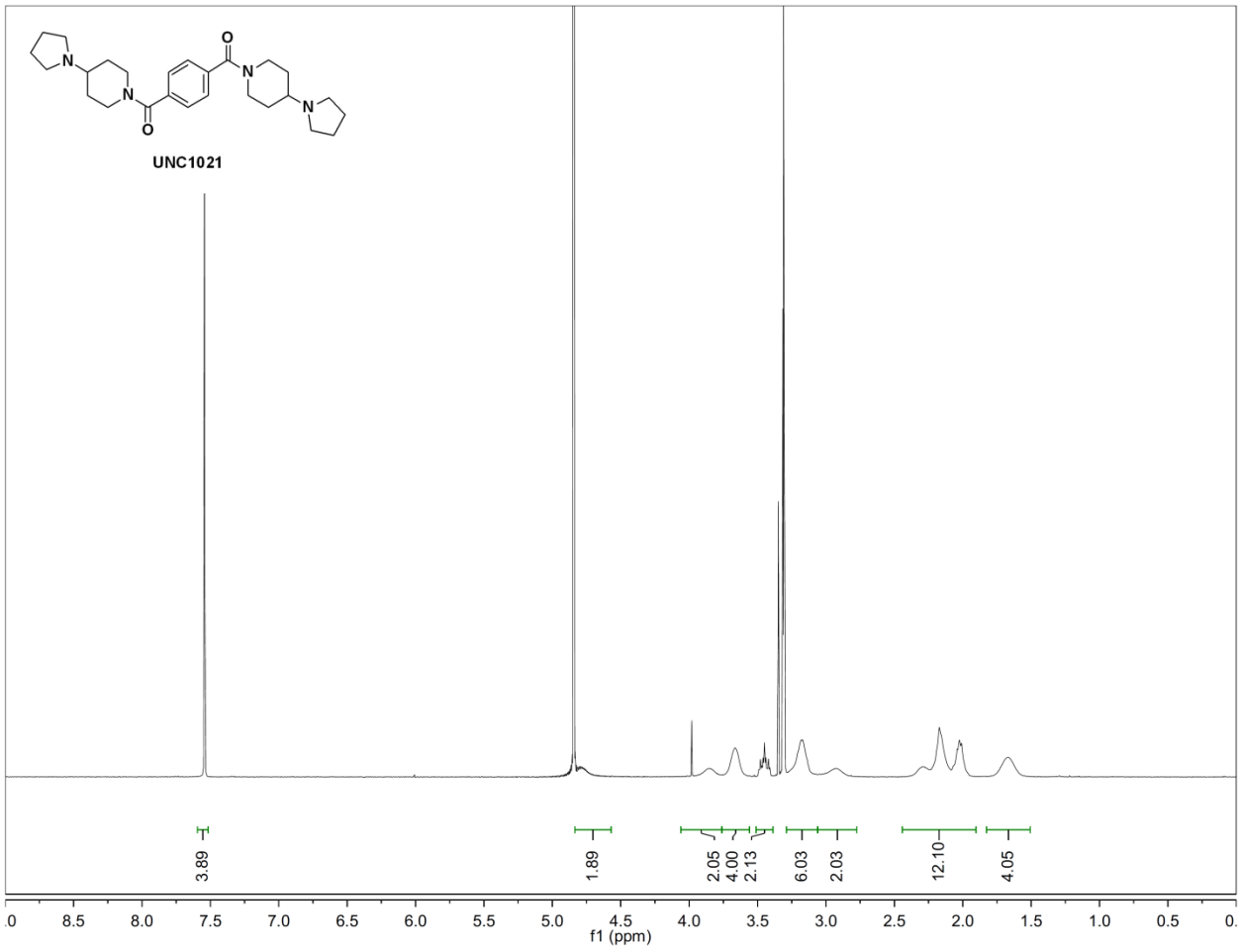

Supplementary Figure 26. LCMS trace of UNC1021 (2) at 220 and 254 nm.

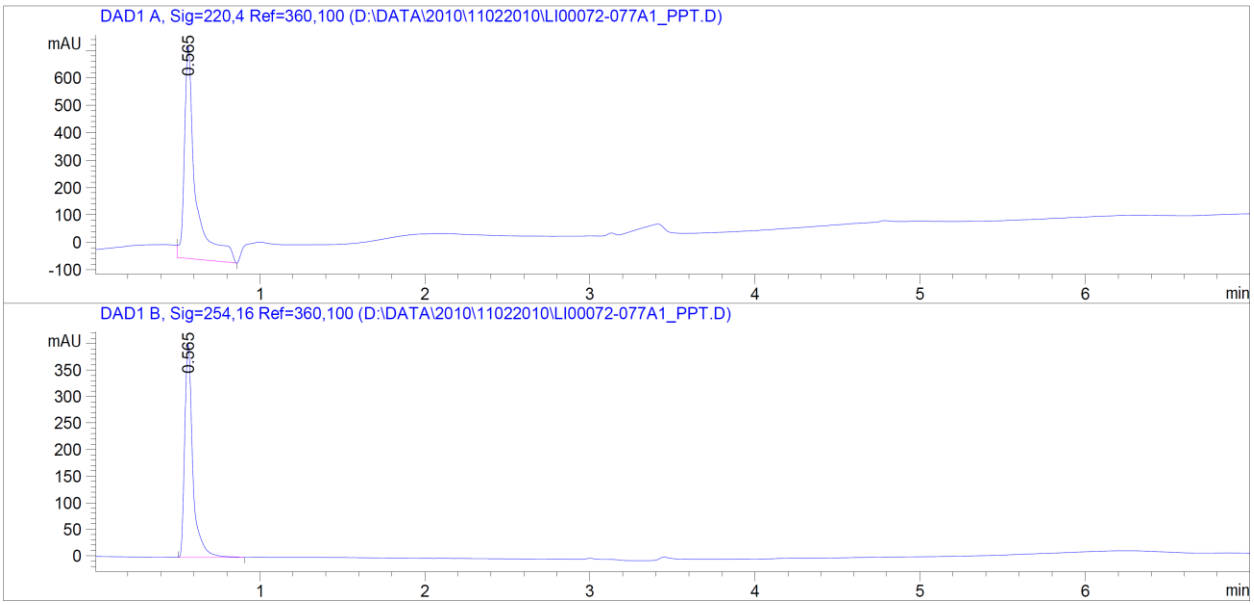

Supplementary Figure 27. ^{1}H NMR spectrum of UNC1079 (3) as a TFA salt. Signal broadening is observed, particularly when the compound exists as a TFA salt, due to slow rotation of the amide bonds on the NMR timescale.

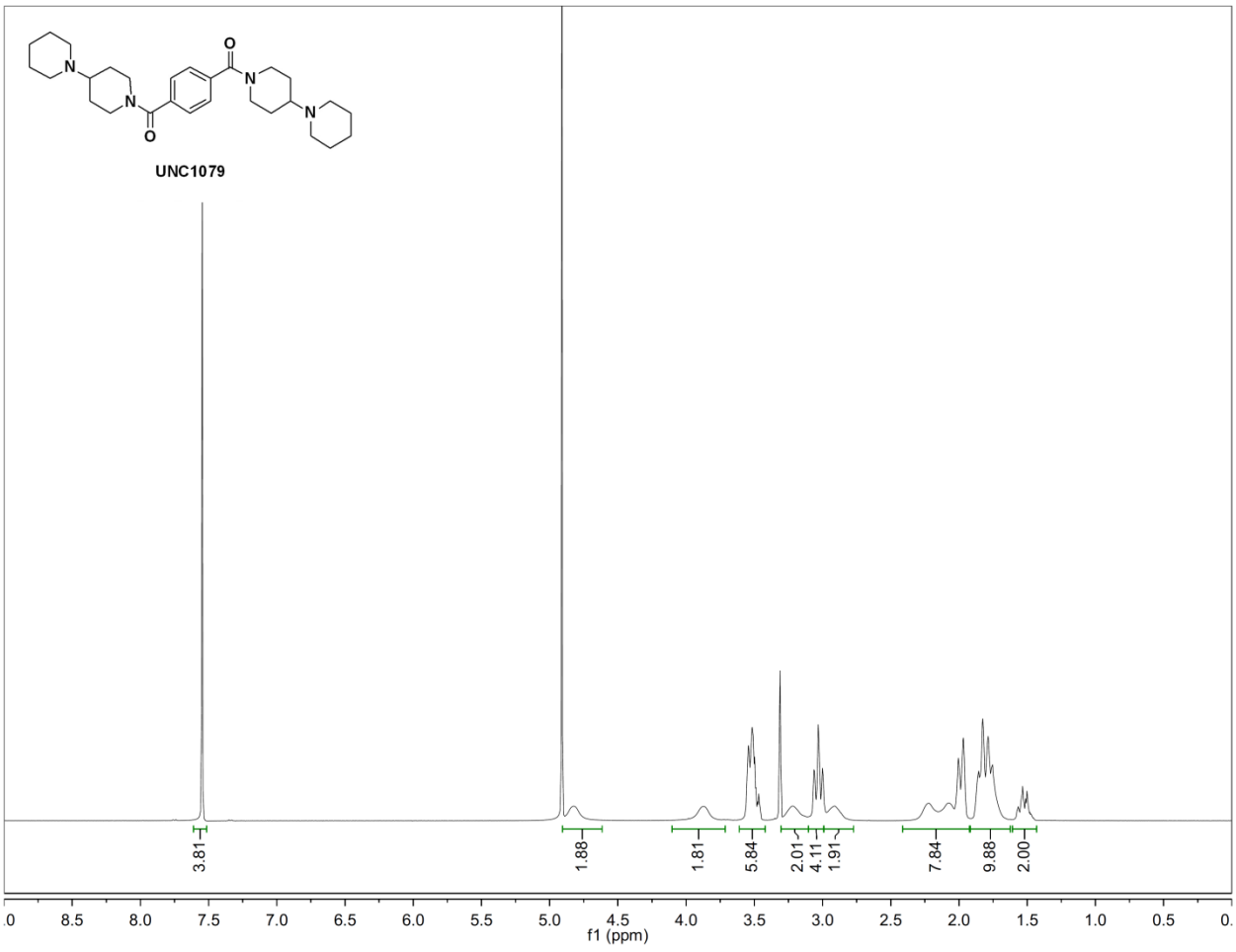

Supplementary Figure 28. LCMS trace of UNC1079 (3) at 220 and 254 nm.

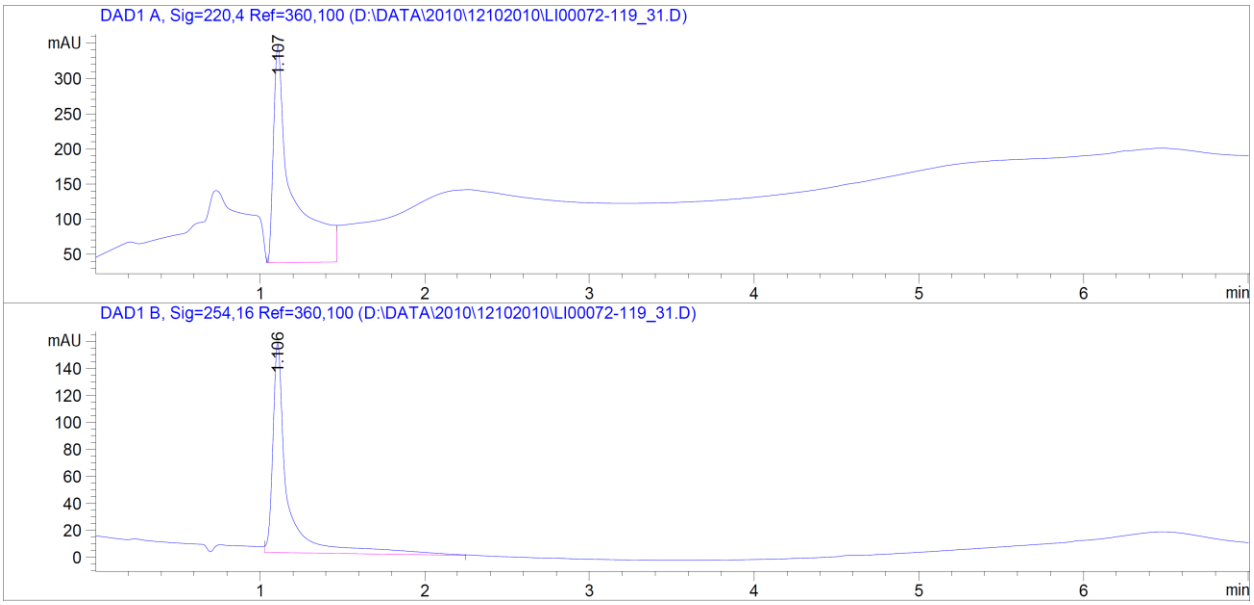

Supplementary Figure 29. ^{1}H NMR spectrum of biotin-1215 (4) as a TFA salt. Signal broadening is observed, particularly when the compound exists as a TFA salt, due to slow rotation of the amide bonds on the NMR timescale.

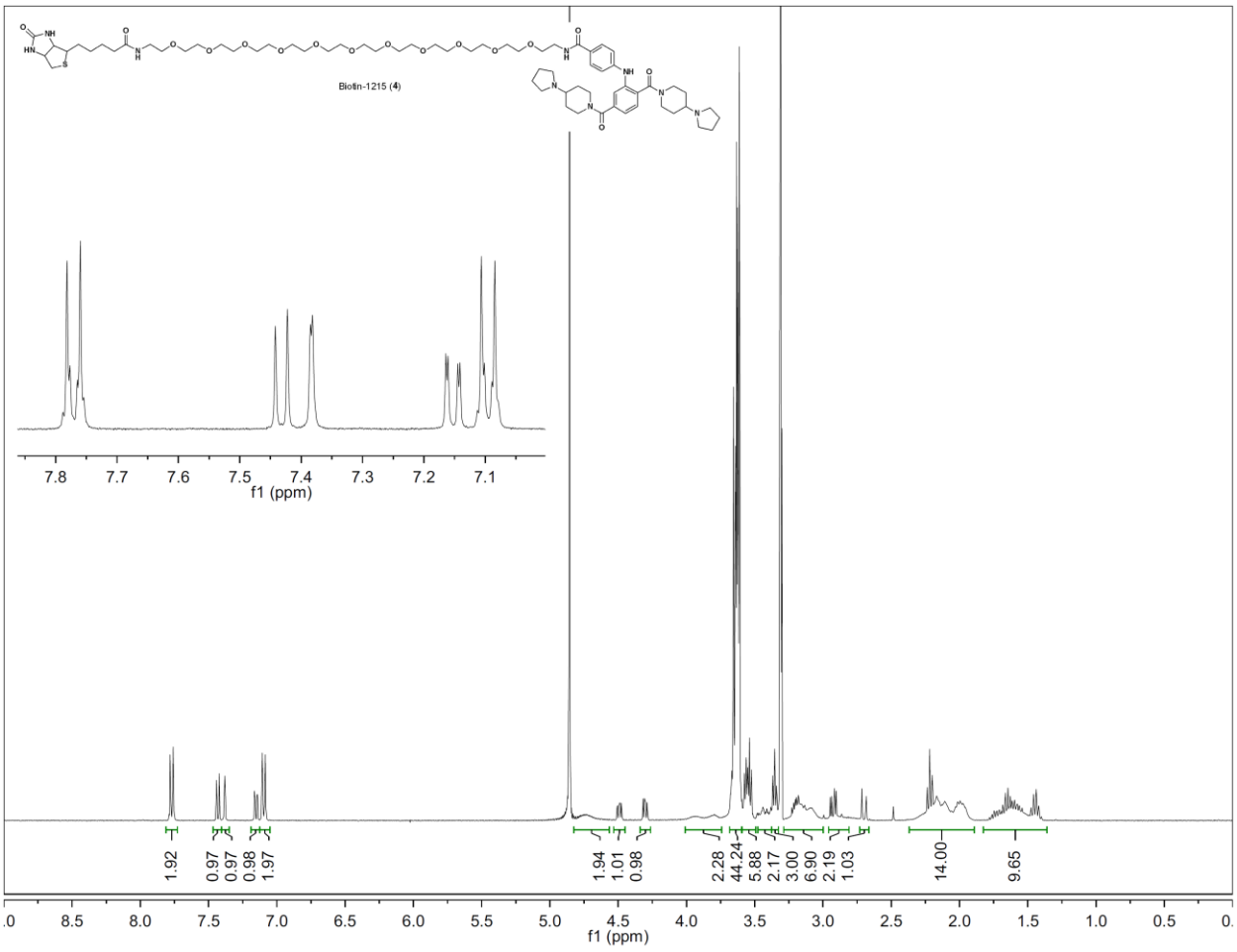

Supplementary Figure 30. ESI-MS of merocyanine-1215 (5).

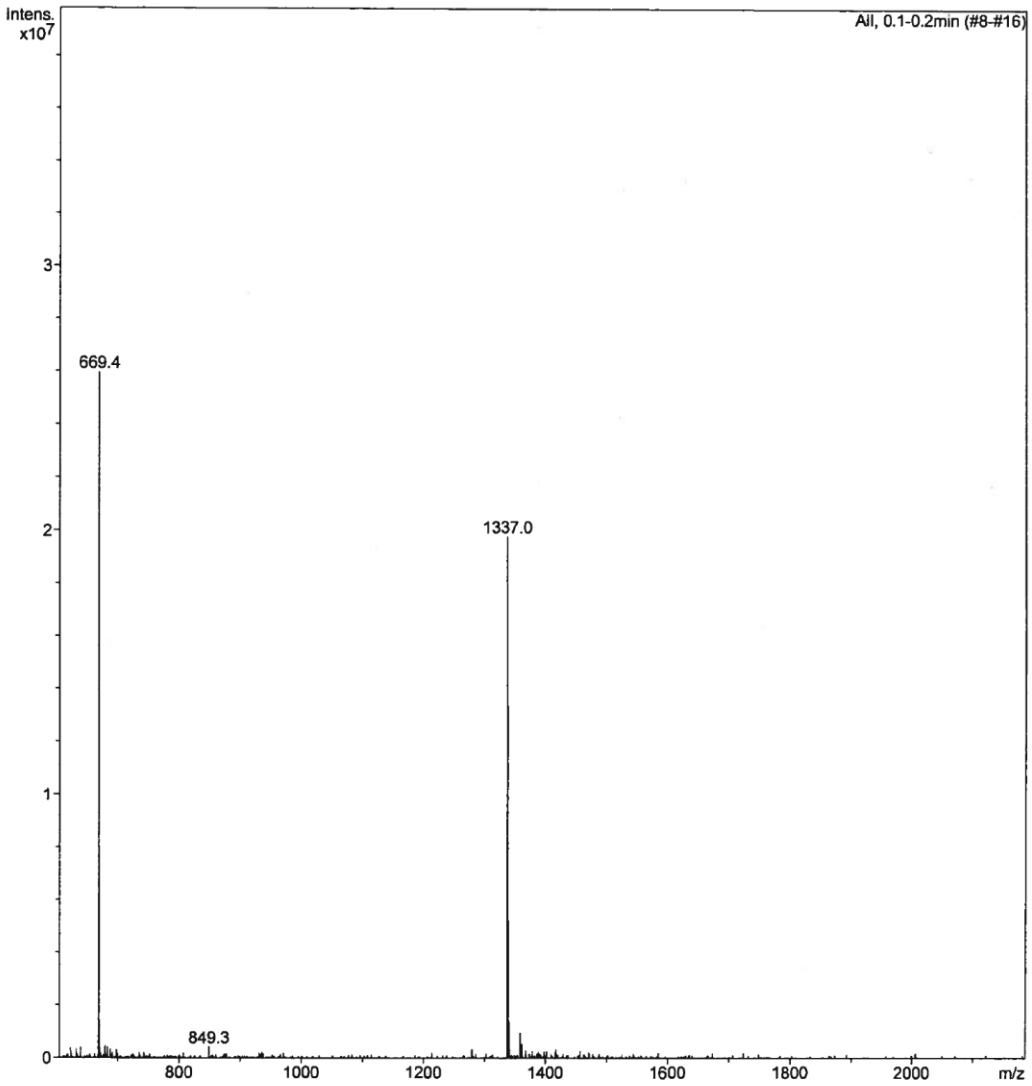

L3MBTL3 protein isoforms. The FLMBT isoform that was used in the cell based assays and in the context of the FLMBT fusion proteins was Q96JM7-2 (below, in red) which is missing exon 3. The numbering chosen in this manuscript corresponds to UniProt ID Q96JM7, the canonical isoform (below, in black). For the 3MBT fusion proteins, residues 168-555 of isoform Q96JM7 were used. Mutants D381A and D274A of isoform Q96JM7 are equivalent to D356A and D249A of isoform Q96JM7-2, respectively.

```
1       MTESASSTSG QEFDVFSVMD WKDGVGTLPG SDLKFRVNEF GALEVITDEN EMENVKKATA
1       MTESASSTSG QEFDVFSVMD WKDGVGTLPG SDLKFRVNEF GALEVITDEN EMENVKKATA

61      TTTWMVPTAQ EAPTSPPSSR PVFPPAYWTS PPGCPTVFSE KTGMPFRLKD PVKVEGLQFC
61      TTTWMVPTAQ ---------- ---------- ------VFSE KTGMPFRLKD PVKVEGLQFC

121     ENCCQYGNVD ECLSGGNYCS QNCARHIKDK DQKEERDVEE DNEEEDPKCS RKKKPKLSLK
96      ENCCQYGNVD ECLSGGNYCS QNCARHIKDK DQKEERDVEE DNEEEDPKCS RKKKPKLSLK

181     ADTKEDGEER DDEMENKQDV RILRGSQRAR RKRRGDSAVL KQGLPPKGKK AWCWASYLEE
156     ADTKEDGEER DDEMENKQDV RILRGSQRAR RKRRGDSAVL KQGLPPKGKK AWCWASYLEE

241     EKAVAVPAKL FKEHQSFPYN KNGFKVGMKL EGVDPEHQSV YCVLTVAEVC GYRIKLHFDG
216     EKAVAVPAKL FKEHQSFPYN KNGFKVGMKL EGVDPEHQSV YCVLTVAEVC GYRIKLHFDG

301     YSDCYDFWVN ADALDIHPVG WCEKTGHKLH PPKGYKEEEF NWQTYLKTCK AQAAPKSLFE
276     YSDCYDFWVN ADALDIHPVG WCEKTGHKLH PPKGYKEEEF NWQTYLKTCK AQAAPKSLFE

361     NQNITVIPSG FRVGMKLEAV DKKNPSFICV ATVTDMVDNR FLVHFDNWDE SYDYWCEASS
336     NQNITVIPSG FRVGMKLEAV DKKNPSFICV ATVTDMVDNR FLVHFDNWDE SYDYWCEASS

421     PHIHPVGWCK EHRRTLITPP GYPNVKHFSW DKYLEETNSL PAPARAFKVK PPHGFQKKMK
396     PHIHPVGWCK EHRRTLITPP GYPNVKHFSW DKYLEETNSL PAPARAFKVK PPHGFQKKMK

481     LEVVDKRNPM FIRVATVADT DDHRVKVHFD GWNNCYDYWI DADSPDIHPV GWCSKTGHPL
456     LEVVDKRNPM FIRVATVADT DDHRVKVHFD GWNNCYDYWI DADSPDIHPV GWCSKTGHPL

541     QPPLSPLELM EASEHGGCST PGCKGIGHFK RARHLGPHSA ANCPYSEINL NKDRIFPDRL
516     QPPLSPLELM EASEHGGCST PGCKGIGHFK RARHLGPHSA ANCPYSEINL NKDRIFPDRL

601     SGEMPPASPS FPRNKRTDAN ESSSSPEIRD QHADDVKEDF EERTESEMRT SHEARGAREE
576     SGEMPPASPS FPRNKRTDAN ESSSSPEIRD QHADDVKEDF EERTESEMRT SHEARGAREE

661     PTVQQAQRRS AVFLSFKSPI PCLPLRWEQQ SKLLPTVAGI PASKVSKWST DEVSEFIQSL
636     PTVQQAQRRS AVFLSFKSPI PCLPLRWEQQ SKLLPTVAGI PASKVSKWST DEVSEFIQSL

721     PGCEEHGKVF KDEQIDGEAF LLMTQTDIVK IMSIKLGPAL KIFNSILMFK AAEKNSHNEL
696     PGCEEHGKVF KDEQIDGEAF LLMTQTDIVK IMSIKLGPAL KIFNSILMFK AAEKNSHNEL
```

Supplementary Table 1. Activity of UNC1021, UNC1215, and UNC1079 against a panel of Kme reader proteins.

Alphascreen IC_{50} [μM][a]	L3MBTL1	L3MBTL3	L3MBTL4	SFMBT	MBTD1	CBX7	53BP1	UHRF1	PHF23	JARID1A
	MBT domains					Chromo Domain	Tudor Domains		PHD Fingers	
UNC1021	**3** (R^2 = 0.93, n = 44)	**0.04** (R^2 = 0.94, n = 44)	**16** (R^2 = 0.72, n = 35)	**> 30** (n = 33)	**11** (R^2 = 0.85, n = 29)	**> 30** (n = 31)	**17** (R^2 = 0.76, n = 45)	**>30** (n = 33)	**>30** (n = 6)	**>30** (n = 6)
UNC1215	**2** (R^2 = 0.93, n = 17)	**0.04** (R^2 = 0.93, n = 17)	**11** (R^2 = 0.63, n = 21)	**> 30** (n = 18)	**6** (R^2 = 0.71, n = 11)	**> 30** (n = 19)	**4** (R^2 = 0.90, n = 12)	**>30** (n = 18)	**>30** (n = 15)	**>30** (n = 15)
UNC1079	**> 30** (n = 6)	**21** (R^2 = 0.72, n = 6)	**>30** (n = 6)	**>30** (n = 5)	**3** (R^2 = 0.91, n = 5)	**>30** (n = 5)	**> 30** (n = 8)	**>30** (n = 5)	**>30** (n = 6)	**>30** (n = 6)

[a] The data for the IC_{50} values was calculated from n replicate runs; data points for each compound concentration were averaged and plotted using 4-parameters curve fitting. R^2 is a statistical estimate of goodness-of-fit.

Supplementary Table 2. Molecular profiling of UNC1215 (see Supplementary Table 1 for Alphascreen data against additional methyl-lysine reader proteins).

Target Category	Target Activity		
Within methyl-lysine reader target family	**Target**	**IC_{50} (μM)**[a]	**K_d (μM)**[b]
	L3MBTL3	0.04 (R^2 = 0.93, n = 17)	0.12 ± 0.11 (n = 5)
	L3MBTL1	2 (R^2 = 0.93, n = 17)	9.4 ± 1.7 (n = 3)
	53BP1	4 (R^2 = 0.90, n = 12)	> 31 (n = 2)
	PHF20 Tudor	NT	5.6 ± 0.49 (n = 2)
	SPF30 (*S.p.*) Tudor	NT	Very weak binding
	PHF20L1 Tudor	NT	> 13 (n = 1)
	PHF20L1 MBT	NT	Very weak binding
	MRG15	NT	28.9 ± 0.2 (n = 2)
Histone methyltransferases	< 50% inhibition at 250 μM versus 10 targets[c]		
Bromodomains	T_m shift < 0.5 °C at 10 μM versus 12 targets[d]		
Histone demethylases	T_m shift < 0.1 °C at 50 μM versus 15 targets[d]		
NIMH Psychoactive Drug Screening Program Selectivity Panel	< 50% inhibition at 10 μM versus 35 targets > 50% inhibition at 10 μM versus 8 targets		
	Target	**K_i (μM)**[e,h]	**IC_{50} (μM)**[h]
	Alpha 2C	0.86	NT
	DAT	> 10	NT
	KOR	4.0	NT
	M1	0.097	3.6[f]
	M2	0.072	30% at 30 μM[g]
	M3	0.89	NT
	M4	0.40	NT
	M5	4.3	NT
Kinase Selectivity Panel	< 15% inhibition at 10 μM versus 49 kinases		
	Target	% Inhibition at 10 μM	
	FLT3	64%	

[a]Alphascreen assays results. [b]ITC results. [c]Radioactive SAM methyl transfer assay results. [d]Differential scanning fluorimetry results. [e]Radioligand binding assay results. [f]Ca^{2+} mobilization assay results. [g]cAMP biosensor assay results. [h]Confidence intervals not reported, n = 1.

Supplementary Table 3. AlphaScreen proteins and peptide substrates.

Protein	Peptide	Peptide sequence	Protein final concentration in 10 µL	Peptide final concentration in 10 µL
L3MBTL1	H4K20Me1	Biotin-AHA-KGGAKRHRK(Me1)VLRDNIQ-COOH	50 nM	150 nM
L3MBTL3	H4K20Me2	Biotin-AHX-KGGAKRHRK(Me2)VLRDNIQ-OH	200 nM	150 nM
L3MBTL4	H2AK36Me1	Biotin-AHA-GRVHRLLRK(Me1)GNYSER-COOH	100 nM	150 nM
MBTD1	H4K20Me1	Biotin-AHA-KGGAKRHRK(Me1)VLRDNIQ-COOH	100 nM	150 nM
SFMBT1	H3K9Me1	Biotin-AHA-ARTKQTARK(Me1)STGGKA-COOH	100 nM	150 nM
CBX7-Flag	H3K9Me3	ARTKQTARK(Me3)STGGKAPRKQL-K(Biotin)-NH2	100 nM	150 nM
53BP1	H4K20Me2	Biotin-AHX-KGGAKRHRK(Me2)VLRDNIQ-OH	100 nM	150 nM
UHRF1	H3K9Me3	Biotin-AHA-ARTKQTARK(Me3)STGGKA-COOH	100 nM	150 nM
PHF23	H3K4Me3	NH2-ARTK(Me3)QTARKSTGGKAPRKQYT-K(Biotin)	60 nM	100 nM
JARID1A	H3K4Me3	NH2-ARTK(Me3)QTARKSTGGKAPRKQYT-K(Biotin)	10 nM	30 nM

Supplementary Table 4. Data collection and refinement statistics (molecular replacement).

Data collection	
Space group	C2
Cell dimensions	
a, *b*, *c* (Å)	228.03, 54.37, 65.55
α, β, γ (°)	90.00, 97.11, 90.00
Resolution (Å)	45.57-2.55 (2.69-2.55) *
R_{merge}	0.062 (0.981)
$I / \sigma I$	15.3 (1.3)
Completeness (%)	99.2 (98.3)
Redundancy	3.7 (3.5)
Refinement	
Resolution (Å)	44.11-2.55
No. reflections work / free	24740 / 1330
R_{work} / R_{free}	0.195 / 0.259
No. atoms	
Protein	4697
Ligand/ion	78
Water	none
B-factors†	
Protein	77.0
Ligand/ion	65.5
Water	n/a
R.m.s. deviations	
Bond lengths (Å)	0.010
Bond angles (°)	1.1

*Highest-resolution shell is shown in parentheses.
†Calculated with program MOLEMAN (G. Kleywegt).

Supplementary Table 5. Targets in the bromodomain, lysine demethylase, kinase selectivity, and NIMH psychoactive drug screen program comprehensive selectivity panels.

Kinase Selectivity Panel	Bromodomain Selectivity Panel	Lysine Demethylase Selectivity Panel	NIMH Psychoactive Drug Screen Program Comprehensive Panel
ABL	BAZ2B	JMJD2A	5-HT_{1A}
CSK	BRD2A~1	JMJD2CA	5-HT_{1B}
EGFR	BRD2A~2	JMJD2D	5-HT_{1D}
EPHA2	BRD3A~1	JMJD2E	5-HT_{1E}
EPHB4	BRD3A~2	JMJD3	5-HT_{2A}
FGFR1	BRD4A~1	JMJD1AA	5-HT_{2B}
FLT3	BRD4A~2	FBXL11	5-HT_{2C}
IGF1R	BRDTA	PHF8	5-HT_{3}
ITK	CREBBPA	KIAA1718c	5-HT_{5A}
JAK3	LOC93349A	FIH	5-HT_{6}
KDR	PB1A~5	MINAB	5-HT_{7}
LCK	PCAFA	NO66	α_{1A}
MET		JMJD6	α_{1B}
PDGFRα		JMJD5	α_{1D}
PYK2		ASPHA	α_{2A}
SRC			α_{2B}
SYK			α_{2C}
TIE2			β_{1}
TRKA			β_{2}
TYRO3			β_{3}
AKT1			D_{1}
AMPKα1/β1/γ1			D_{2}
AurA			D_{3}
CaMK4			D_{4}
CDK2/CycA2			D_{5}
CHK1			Dopamine transporter (DAT)

CK1ε			$GABA_A$, muscimol, central
DAPK1			$GABA_A$, flunitrazepam, central
DYRK1B			H_1
Erk2			H_2
GSK3β			H_3
HGK			H_4
IKKβ			M_1
IRAK4			M_2
JNK2			M_3
MAPKAPK2			M_4
MST1			M_5
NEK2			Norepinephrine transporter (NET)
p38α			δOR
p70S6K			κOR
PAK2			μOR
PBK			Peripheral benzodiazepine receptor (PBR)
PDK1			Serotonin transporter (SERT)
PIM1			σ1
PKACα			σ2
PKCα			
PKD2			
ROCK1			
SGK			
TSSK1			

Supplementary Table 6. Half-life and dissociation constant data for the GFP constructs of L3MBTL3.

GFP-FLMBT	Halflife, s	D, Dissociation constant, $\mu m^2/s$
WT	27.1	0.037549815
D274A	18.3	0.055618046
D381A	12.2	0.083699078
Control	26.2	0.038884219
UNC1079 1 µM	28.5	0.035742887
UNC1215 1 µM	19.9	0.051033099
UNC1215 0.5 µM	20.3	0.050251852
UNC1215 0.1 µM	20.1	0.050702541
UNC1215 0.01 µM	23.8	0.042792262
GFP-3MBT	Halflife, s	D, Dissociation constant, $\mu m^2/s$
WT	8.0	0.1272
D274A	6.3	0.16180337
D381A	5.8	0.176132642
Control	7.5	0.136024596
UNC1079 1 µM	8.2	0.123991714
UNC1215 1 µM	3.6	0.284325231
UNC1215 0.5 µM	3.4	0.296244541
UNC1215 0.1 µM	3.3	0.311287856
UNC1215 0.05 µM	6.5	0.156097561
UNC1215 0.01 µM	7.0	0.145892473

Supplementary Table 7. Antibodies to histone marks (top) and other targets (bottom) that were used for co-localization immunofluorescence experiments with GFP-FLMBT and/or GFP-3MBT.

Antibody	Supplier, #
H4K20me3	Abcam ab9053
H3K27me3	Upstate 07-449
H4K20me2	Active Motif 39174
H4K20me1	Active Motif 39728
H2AXgamma	Abcam ab11175
H3K36me3	Abcam ab9050
H3K36me2	Abcam ab9049
H3K79me2	Abcam ab3594
H3K9me3	Abcam ab8898

Antibody	Supplier, #
DNMT1	Abcam ab19905
PML	Abcam ab53773
RNAPII CTD	Abcam ab5408
Fibrilliarin	Abcam ab4566
Sc-35	Abcam ab11826
P53	Cell Signaling Technology 2524
CREST	Provided by Edyta Marcon
RARa	Abcam ab53161

[1] Wigle, T.J. et al. Screening for Inhibitors of Low-Affinity Epigenetic Peptide-Protein Interactions: An AlphaScreenTM-Based Assay for Antagonists of Methyl-Lysine Binding Proteins. *J Biomol Screen* 15, 62-71 (2010).

[2] Pace, C.N., Vajdos, F., Fee, L., Grimsley, G. & Gray, T. How to measure and predict the molar absorption coefficient of a protein. *Protein Sci* 4, 2411-23 (1995).

[3] Herold, J.M. et al. Small-Molecule Ligands of Methyl-Lysine Binding Proteins. *Journal of Medicinal Chemistry* 54, 2504-2511 (2011).

[4] Cui, G. et al. PHF20 is an effector protein of p53 double lysine methylation that stabilizes and activates p53. *Nat Struct Mol Biol* 19, 916-924 (2012).

[5] Kim, J. et al. Tudor, MBT and chromo domains gauge the degree of lysine methylation. *EMBO Rep* 7, 397-403 (2006).

[6] Yang, Y. et al. TDRD3 Is an Effector Molecule for Arginine-Methylated Histone Marks. *Molecular Cell* 40, 1016-1023 (2010).

[7] Fedorov, O., Niesen, F.H. & Knapp, S. Kinase inhibitor selectivity profiling using differential scanning fluorimetry. *Methods Mol Biol* 795, 109-18 (2012).

[8] Christopoulos, A., Parsons, A.M., Lew, M.J. & El-Fakahany, E.E. The assessment of antagonist potency under conditions of transient response kinetics. *Eur J Pharmacol* 382, 217-27 (1999).